Propagation of a Detonation in a Converging Conical Channel

Ivan Hung

Master of Engineering

Department of Mechanical Engineering

McGill University

Montreal, Quebec

15TH AUGUST, 2017

A thesis submitted to McGill University

in partial fulfillment of the requirements of the degree of

Master of Engineering - Mechanical Engineering (Thesis)

Contents

Abstract

The presented work is an experimental study of detonation propagation in a converging conical channel. We explore the amplification of the detonation wave in a conical tube with a small angle of convergence. Experiments were carried out in a detonation tube which has a straight, constant area cylindrical section with inner diameter of 6.35 cm and length of 3 m. At the end of the cylindrical tube is the conical tube. A Chapman-Jouguet (C-J) detonation wave is first established in the constant area portion of the tube prior to entering the converging section. Two explosive mixtures: stoichiometric acetylene-oxygen mixture ($C_2H_2 + 2.5O_2$) and acetylene-oxygen mixture with 70% argon dilution ($C_2H_2 + 2.5O_2 + 70\%$ Ar) were used. The initial pressure range of the experiments are from 0.5 kPa to 10 kPa and from 4 kPa to 16 kPa respectively for the two mixtures. It was found that for cone angles $\lesssim 20°$, the Mach stem curves to merge with the incident detonation to give a smooth continuous detonation front. The reflected shock also degenerates into a series of compression waves in the triple point region. In the present study, the detonation velocity is measured via ionization probes spacing periodically in both the constant area section as well as the converging conical section. Smoked foils are also used to determine the detonation cell structure in both the straight as well as the converging sections of the detonation tube. A PCB Piezotronics Pressure Sensor is also placed at the end of the conical section to measure the reflected pressure of the detonation. A continuous increase in the detonation velocity and decrease in the cell size were observed as the detonation propagates into the conical tube. Smoked foil records indicate the absence of a distinct triple point trajectory separating the Mach stem from the incident wave, indicating a smooth continuous converging detonation front is obtained

Abrégé

Cette thèse rapporte les résultats d'une étude expérimentale sur la propagation de détonations dans un tube conique convergent. L'intérêt est particulièrement porté sur leurs amplifications alors qu'elles se propagent dans un tube conique à petit angle. Les expériences ont été conduites dans un tube à détonation formé de deux sections distinctes : un tube droit d'une longueur total de 3m avec un diamètre de 6.35 cm qui est connecté à la toute fin à un tube conique convergent. Une détonation Chapman-Jouguet (C-J) est initialement obtenue dans la première section, un peu avant la section convergente. Deux mélanges explosifs ont été utilisé: un mélange stœchiométrique d'acétylène-oxygène ($\mathrm{C_2H_2 + 2.5O_2}$) et un mélange d'acétylène-oxygène concentré à 70% d'argon ($\mathrm{C_2H_2 + 2.5O_2 + 70\%\ Ar}$). La pression de chaque mélange a été varié de 0.5 kPa à 10 kPa et de 4 kPa à 16 kPa respectivement. Il a été possible de démontrer que pour un cône avec un angle $\lesssim 20°$ le Mach stem, généralement perpendiculaire à la surface sur laquelle il se propage, devient courbe et se confond avec la détonation incidente. Ceci résulte en un détonation d'apparence lisse et continue au lieu d'une détonation avec un point triple défini. L'onde qui est réfléchie dégénère en une série d'onde de compression dans la région du point triple. La vitesse de détonations est mesurée à l'aide de capteurs d'ionisations séparés de manière périodique dans les deux sections du tube à détonation. Afin d'observer la structure cellulaire des détonations, des feuilles fumées en laboratoire ont été placé sur les surfaces internes au bout de la section linéaire de même que sur l'entièreté du tube conique convergent. Un capteur de pression Piezotronics PCB a été inséré à la pointe du tube conique, afin de mesurer la pression lorsque la détonation est réfléchie. Dans la section convergente, il y a une augmentation de la vitesse de détonations accompagné d'une réduction de la taille des cellules. Pour un angle $\lesssim 20°$, les feuilles fumées ont montré l'absence

d’un point triple qui sépare le Mach stem de l’onde incidente ce qui indique alors que le front de détonations et lisse et continue.

List of Figures

Acknowledgements

I would like to first express my most sincere gratitude and appreciation to my supervisor, Professor John Lee. As just a student who recently finished 4 years of undergraduate studies, I feel extremely honored to have the opportunity to work with an internationally well-known researcher in the field of fluid mechanics and detonation. He is always there when I need help and has taught me many things, not only on the research subject on its own but also in life. He provided me with vision, guidance and support not just as a supervisor, but also as a mentor and friend. The experience I had with him does not just deepen my knowledge in the field of fluid mechanics, but will also help me grow as a person in the future and will be forever unforgettable.

I would also like to thank my colleagues in the Shockwave Physics Group for creating a rigorous, yet pleasant, atmosphere in the lab. Their constant assistance accompanied my two years of research and has made the experience much more enjoyable. A special word of gratitude, also, to our technician Andy Hofmann and the Machine Tool Lab technicians, for their tremendous help on machining different components for the experiments with high quality.

Last but not least, I would also like to thank my family at home for their wordless support throughout my life during my ups and downs and allowing me to focus on my education and research without worries. Their continuous support and encouragement inspire me to go beyond myself and keep persevering to pursue my goals.

Chapter 1 : Introduction

The generation of implosions or converging shocks or detonations is of interest because they can produce very high pressure and temperature. There have been numerous past studies on converging shock waves, but there have been very few on converging detonations. Converging cylindrical detonations were studied by Lee *et al.* [1] using a diffraction plate to “turn” a diverging cylindrical detonation to form a converging detonation on the other side of the diffraction plate. A later photographic observation on cylindrical imploding detonations using Schlieren photography on a similar experimental setup was carried out and a smooth cylindrical detonation wave front was observed after a transition from a polygonal shaped wave front. Similar studies by Fujiwara *et al.* [2] also exploited the diffraction plate method develop by Lee *et al.* [1] The diffraction plate is limited to producing converging cylindrical detonations and cannot be used to generate spherical converging detonations. Terao *et al.* [3] also studied spherical and cylindrical imploding detonations using a convergent hemisphere space and the results showed a greater increase in pressure of the imploding detonation than predicted. Matsuo [4] amongst only a few others have studied converging detonations.

Oran *et al.* [5] studied numerically the stability on cylindrically imploding detonation waves and the results showed quantitatively agreement with the Chester [6]-Chisnell [7]-Whitham [8] (CCW) theory. Jiang *et al.* [9] conducted a numerical study on spherically converging detonations and obtained an extremely high post-detonation flow state due to continuous chemical energy releases and area convergence. It was found that chemical energy release was responsible for the increase for the post-detonation state during the majority of the converging process until when it got very close to the focal point while beyond this point, further strengthening was mainly due to area convergence.

However, due to instability, it is very difficult to generate a symmetrical cylindrical or spherical converging detonation. It has been shown in recent studies [10] [11] [12] that as detonation waves propagate into an area converging channel with small angle of convergence, a smooth converging detonation can be obtained, as shown in Fig. 3. In the present study, we investigate the properties of converging detonations propagating in a small angle conical tube.

The propagation of a detonation wave into a two or three-dimensional converging channel results in two types of reflection: a regular reflection, and a Mach reflection, depending on the angle of convergence. Regular reflection is observed when the wedge or cone angle is larger than some critical value. This is illustrated in Fig. 1.

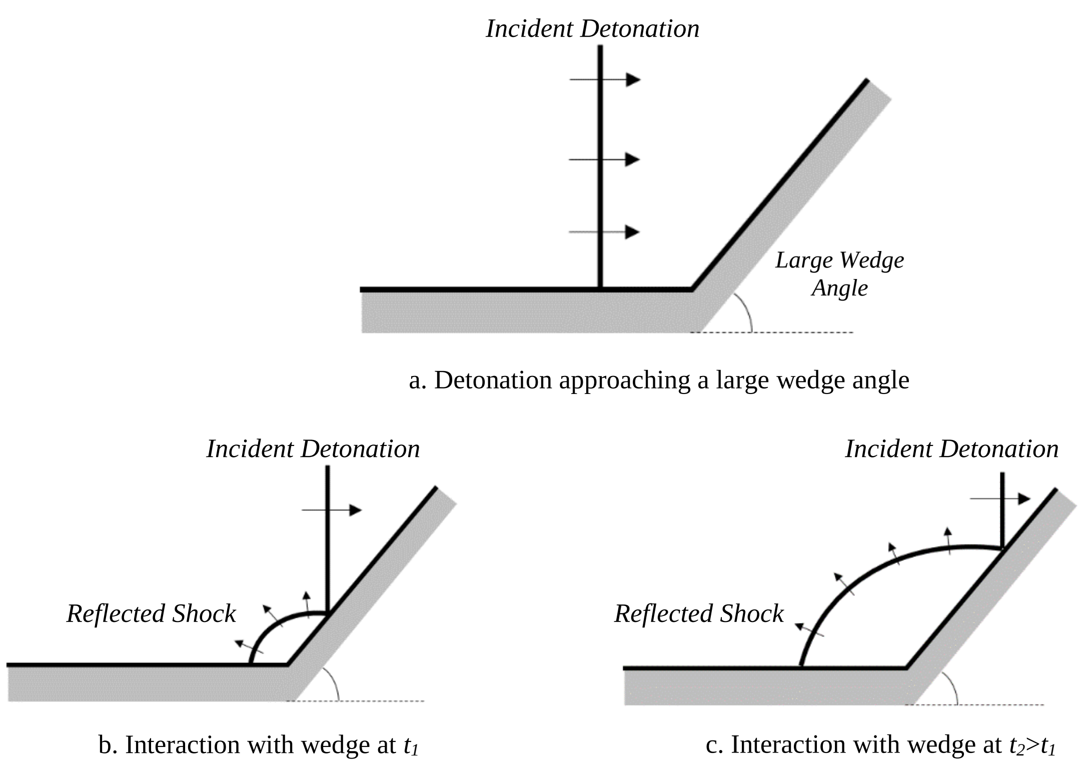

a. Detonation approaching a large wedge angle

b. Interaction with wedge at t_1

c. Interaction with wedge at $t_2 > t_1$

Figure 1: Regular Reflection at Large Wedge Angle

For angles less than the critical angle, triple shock Mach reflection is obtained. In addition to the incident, reflected wave and the Mach stem, a shear layer is also obtained. This is illustrated in Fig. 2.

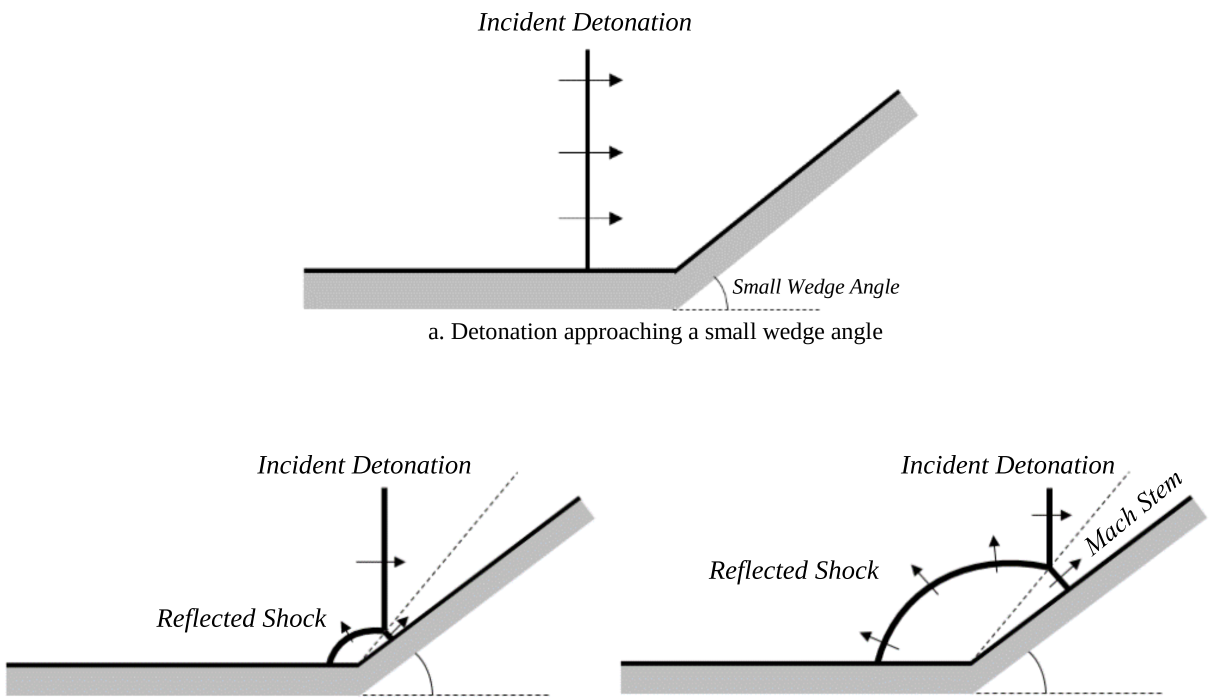

a. Detonation approaching a small wedge angle

b. Interaction with wedge at t_1

c. Interaction with wedge at $t_2>t_1$

Figure 2: Mach reflection at Small Wedge Angle

The Mach stem is stronger than the incident wave. Thus, the strengthening of the detonation in the channel is periodic as triple point reflects back and forth from the centerline and the wall.

In the previous studies of detonation propagation up a wedge by Guo *et al.* [12], Thomas *et al.* [13] and Fortin *et al.* [10], it was found that when the wedge angle is much smaller than the critical angle, e.g. 20°, the Mach stem becomes curved and merges smoothly with the incident wave to form a curve front. The triple point region becomes dispersed and the reflected shock degenerates into a series of compression waves. Therefore, a continuous curved front can be obtained.

However, the strength varies along the curved front from the wall to the centerline, as illustrated in Fig. 3.

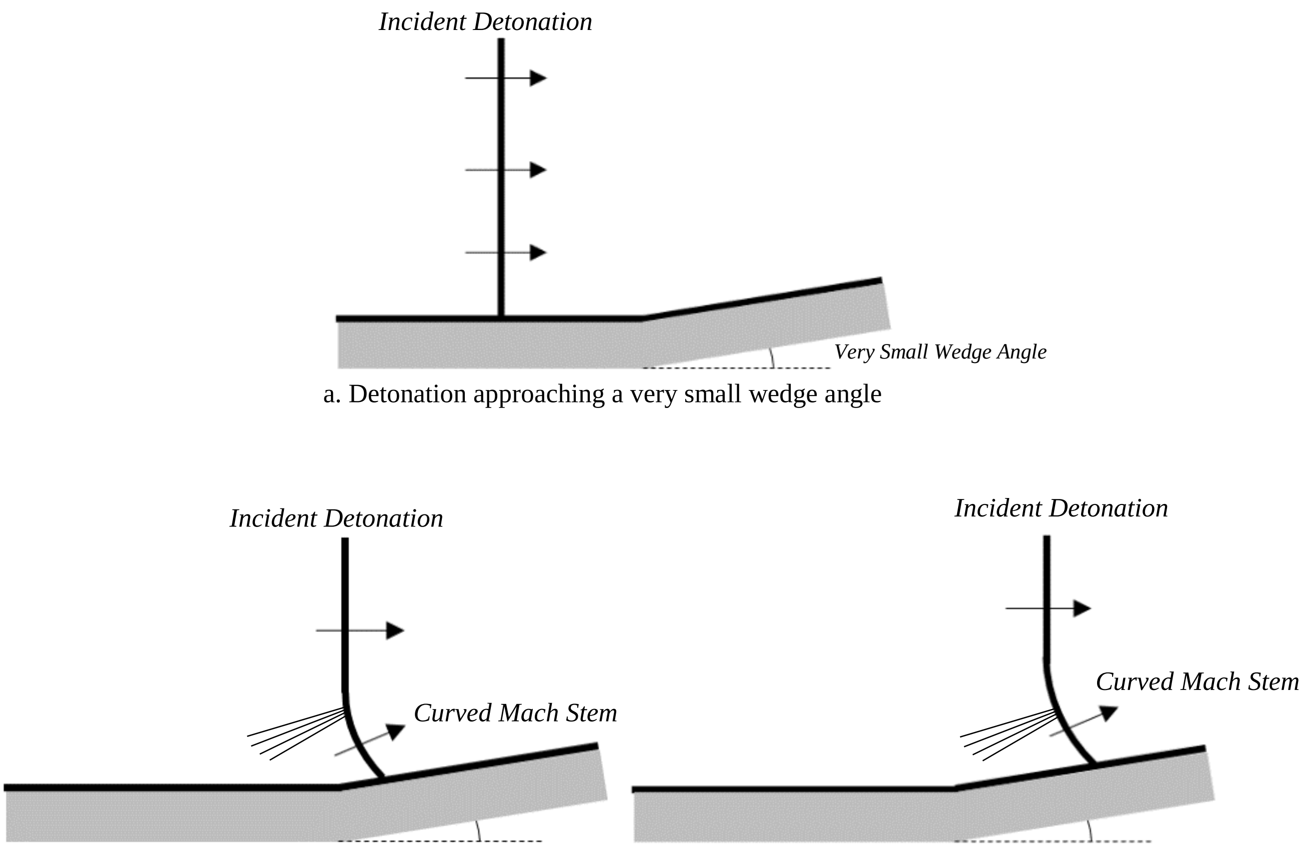

a. Detonation approaching a very small wedge angle

b. Interaction with wedge at t_1

c. Interaction with wedge at $t_2 > t_1$

Figure 3: Curved Wave Front at Very Small Wedge Angle

There has been a number of previous studies on propagation of shock waves in a converging channel. The propagation of strong shock waves in a two-dimensional converging channel was studied by Belokon *et al.* [14] The strengthening of the Mach stem take place discontinuously as the triple point reflects periodically from the wall and the axis, as illustrated in Fig. 4

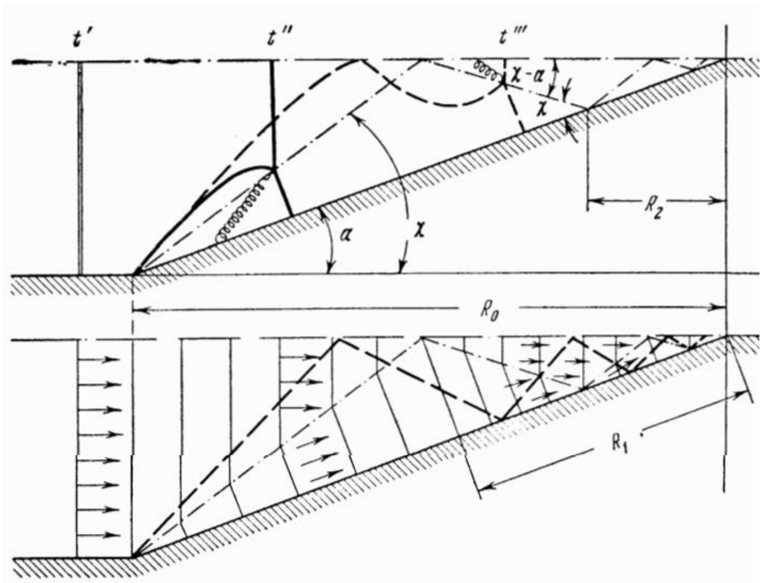

Figure 4: Repeated Mach Reflections*[14]*

Belokon *et al.* observed a significant increase in temperature and density of the plasma when the wave converges to the vertex of the channel of the order of 100 and 1000 times respectively for the temperature and density respectively.

The propagation of shock waves in a small angle cone of 20° was also studied experimentally by Russell [15]. Air was used as the test gas and initial Mach number varies from approximately 2.5 to 5.5. The initial pressure ranges from 0.5 to 50 mmHg. The results were compared to the CCW (Chester-Chisnell-Whitham) Theory. Russell observed a continuous increase in the shock Mach number to two to three times the initial value at the apex of the cone. A satisfactory agreement with the CCW Theory within a 5% accuracy was reported.

Shock waves propagation in the same conical converging channel with total cone angle of 20° was later studied by Setchell [16] [17]. Stronger initial shock waves with Mach numbers varying from 6.0 to 10.2 were used and argon at initial pressure of 1.5 Torr is used, instead of air. The measured velocity in the conical tube showed that the Mach stem undergoes cyclical reflections in the conical tube until it reaches the cone vertex. The velocity showed a periodic increase, corresponding to multiple Mach reflections, as illustrated in Fig. 6. Apparently for strong shocks in the 20° cone, the triple shock configuration did not degenerate into a continuous curve front.

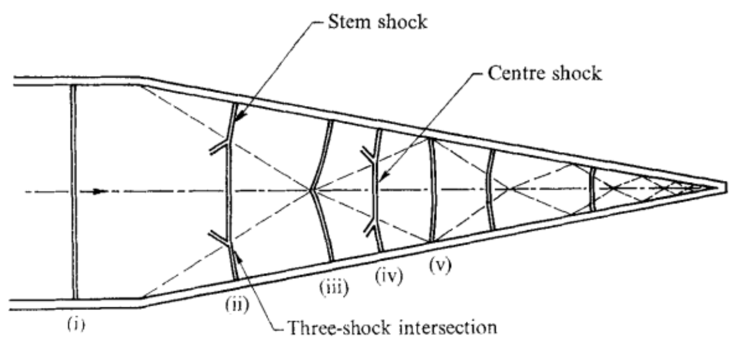

Figure 5: Multiple Mach Reflections of a Shock in a Conical Convergent Channel *[16]*

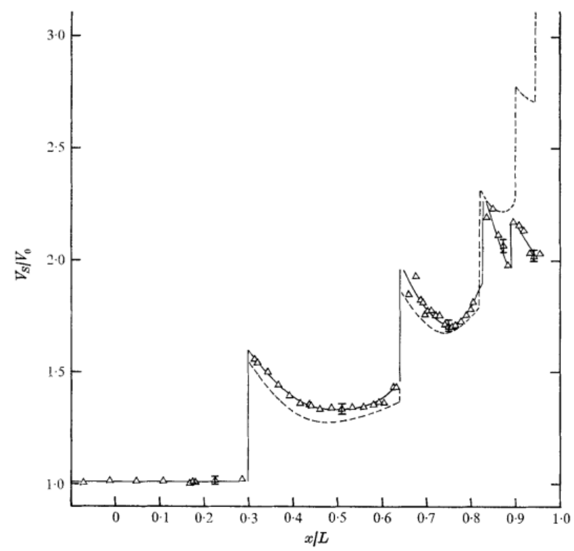

Figure 6: Velocity Profile in Multiple Mach Reflections *[16]*

Milton and Duong [18] also studied experimentally and numerically Mach reflections in a conical converging channel with angles varying from 10° to 30°. Reflections at the centerline and the wall showed a repeated cycle of Mach reflections and the shock Mach number increases in distinct steps, similar to the results of Setchell [16]. Multiple reflection of the triple point trajectory with the axis and the wall observed experimentally showed good agreement with the numerical computations and the previous results [16].

Experiments on converging shock waves were also carried out by Skews *et al.* [19] and Milton *et al.* [20] using a shock tube with a conical section, as shown below in Fig. 7. Numerical simulations were also carried out, as shown in Fig. 8, which shows a complex pattern of the reflection of the shock wave at the end of the conical section.

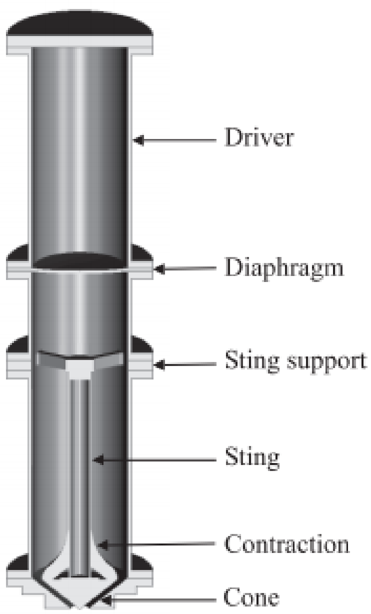

Figure 7: Shock Tube for Imploding Conical Shock *[19]*

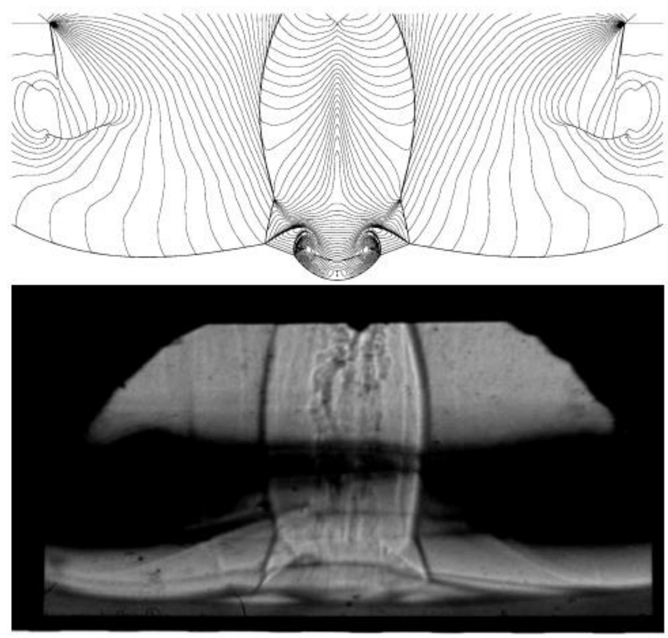

Figure 8: Reflection of an Axisymmetric Oblique Shock*[20]*

Zhai *et al.* [21] also investigated the propagation of shocks waves in a shock tube with a continuously curved wall that varies to a total maximum angle of 15°.

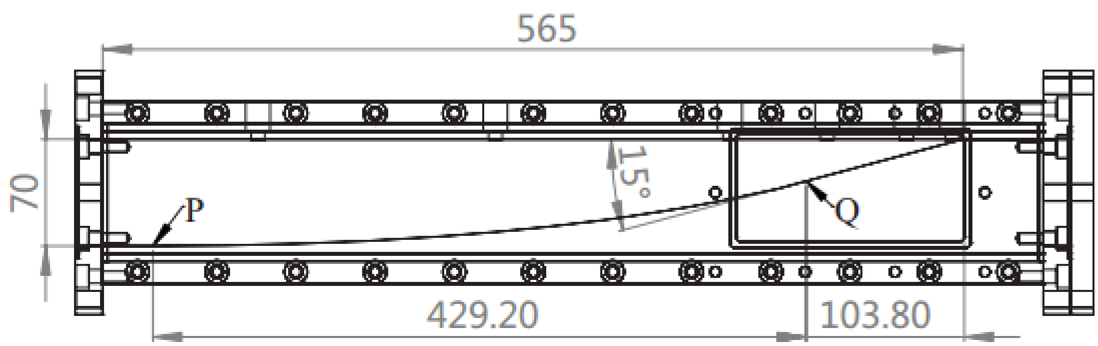

Figure 9: Test Section with Continuously Curved Wall*[21]*

Schlieren photographs were taken and were compared with the results from numerical simulations. The Schlieren photographs show that the initially planar shock transformed into a smooth curved front as it propagates up the channel, as illustrated in Fig. 10.

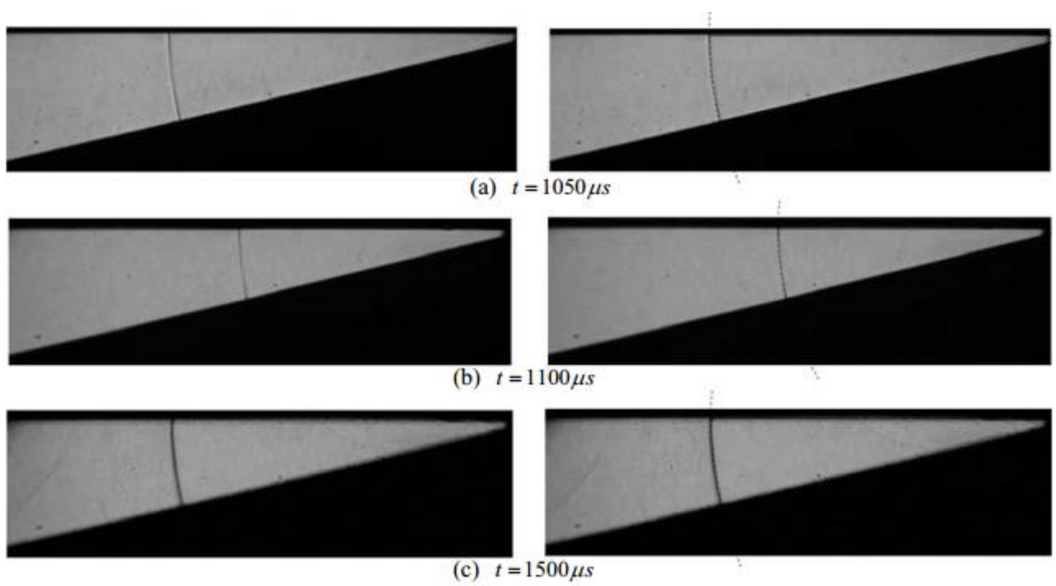

Figure 10: Experimental Schlieren Images in the Converging Section and Comparisons to a Circular Arc *[21]*

The experimental results were found to agree with the numerical simulations based on the CCW Theory. A parametric study on different converging angles indicates a high sensitivity on the variation of channel angles and it is much more difficult to obtain a smooth curved wave front for larger wedge angles. Converging shock waves were also used to ignite a combustible mixture in a converging conical channel by Yang *et al.* [22] Their Schlieren images also indicate a smooth curved wave front is obtained.

A number of previous studies on detonation propagation up a wedge have been carried out.

Guo *et al.* [12] used smoked foils to observe the Mach reflection of detonations in $2H_2 + O_2 + Ar$ mixture. They found that the triple-point trajectory depends primarily on wedge angle, rather than on the initial pressure. Smoked foils of the Mach reflection are shown in Figs. 11 to 13. Mach-stem is found to be overdriven as evidenced by small cell sizes. The triple-point trajectory is found to be an irregular curve, instead of a straight line, due to cellular structure of the detonation wave. In addition, as the wedge angle increases, the triple-point trajectory gets closer and closer to the wedge surface.

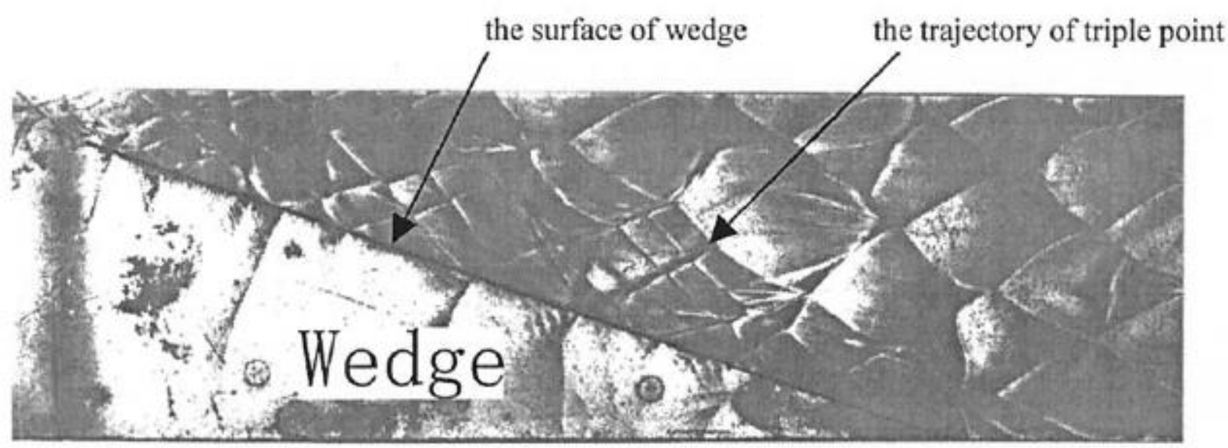

Figure 11: Cellular pattern produced at wedge angle of 19.3°*[12]*

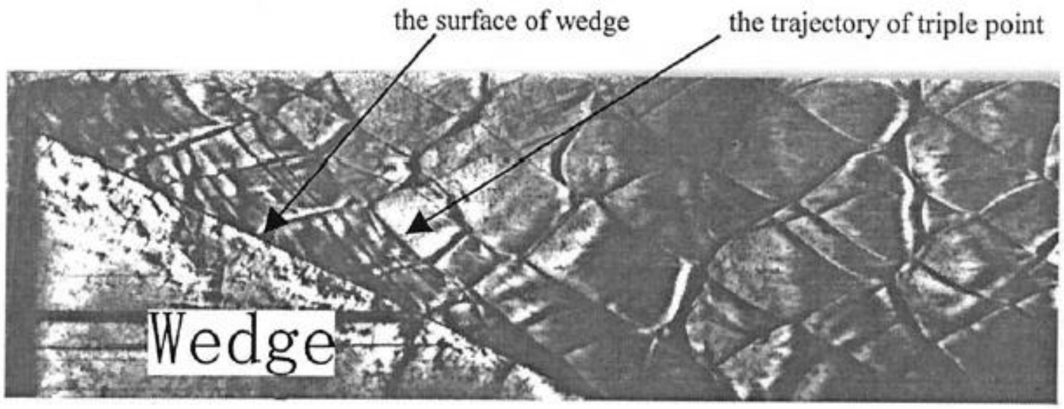

Figure 12: Cellular pattern produced at wedge angle of 26.7° *[12]*

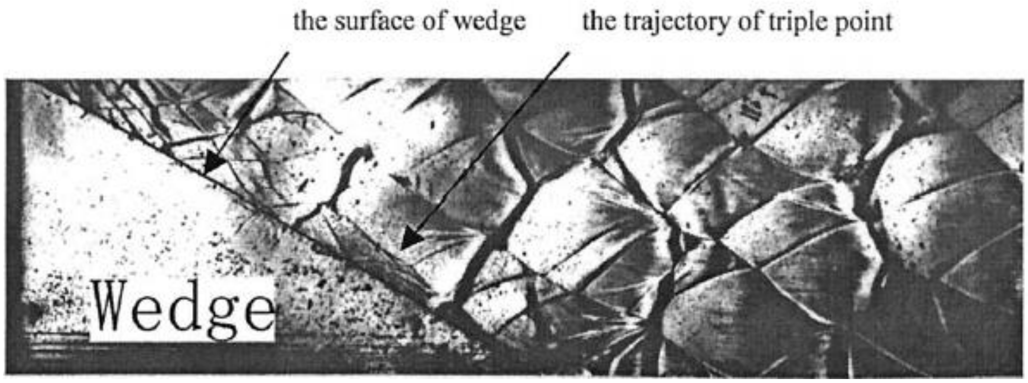

Figure 13: Cellular pattern produced at wedge angle of 30° *[12]*

Thomas *et al.* [13] also studied the interaction of detonations with wedges using smoked foils and Schlieren images. They varied the wedge angles from 14° to 46° and mixture of $2H_2 + O_2 + Ar$ is used. Typical smoked foils are shown in Figs. 14 to 17. A distinct Mach stem could not be identified easily for smaller wedge angles as shown in Fig. 14.

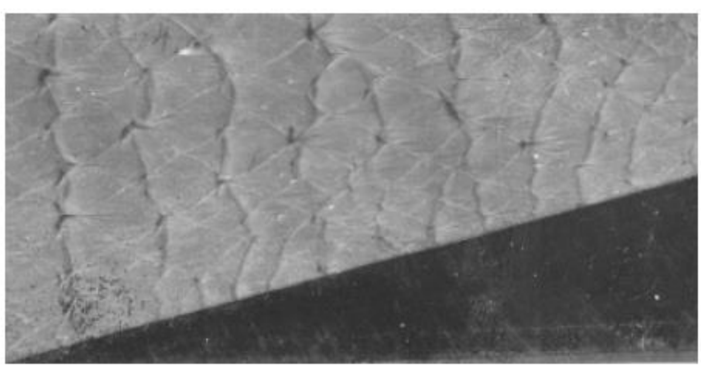

Figure 14: Smoked foil recorded at 14° wedge angle *[13]*

However, the triple point trajectory became clearer at larger wedge angles, as illustrated in Fig. 15 to 17 and the trajectory gets closer to the wedge surface as wedge angle increases.

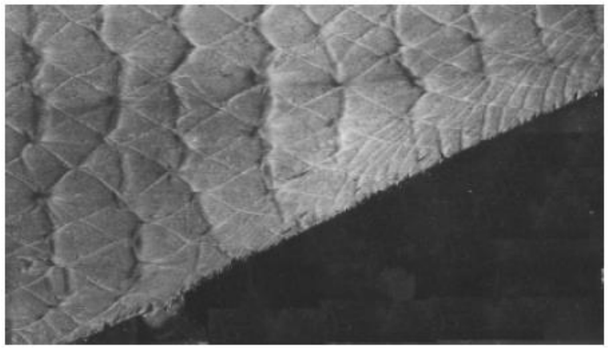

Figure 15: Smoked foil recorded at 25° wedge angle *[13]*

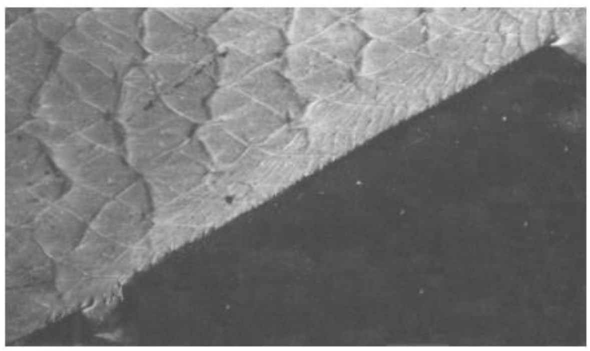

Figure 16: Smoked foil recorded at 30° wedge angle [13]

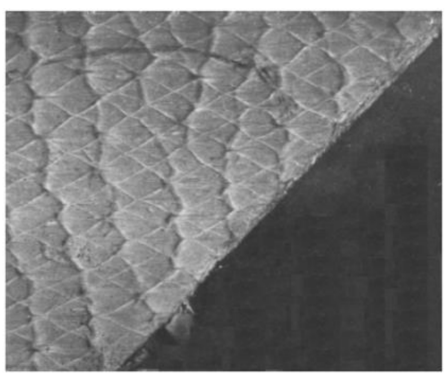

Figure 17: Smoked foil recorded at 46° wedge angle*[13]*

The trajectory of the triple point is defined by the boundary between the larger cells of the incident detonation and the smaller cells in the Mach stem. Schlieren images were also obtained for wedge angles from 20° to 85° in Fig. 18.

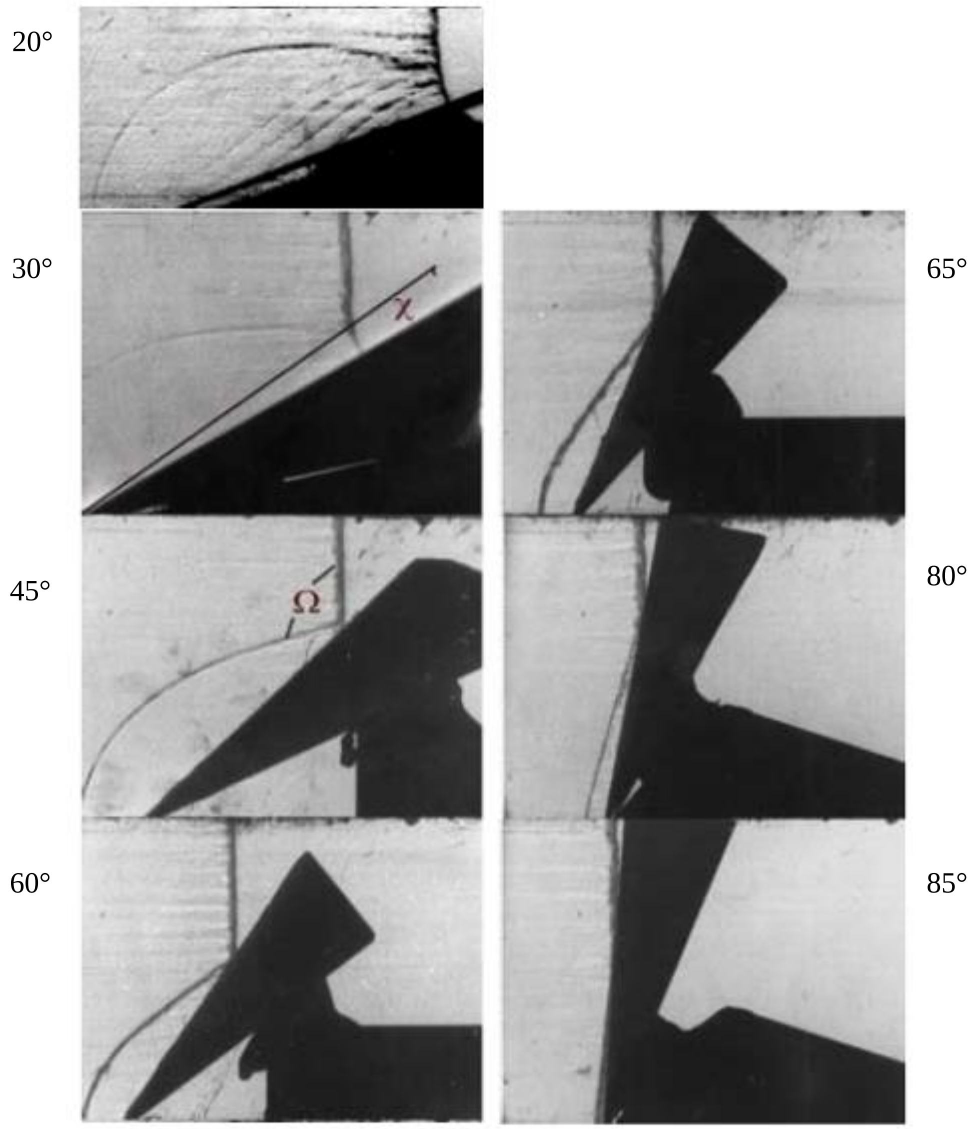

Figure 18: Schlieren Images at Different Wedge Angles: 20°, 30°, 45°, 60° (Left Column) and 65°, 80°, 85 (Right Column) *[13]*

For the smaller angle of 20°, the Mach stem appears to be curved. At wedge angles of 30°, a Mach stem can be identified. At greater wedge angles, the Mach stem cannot be clearly defined as the triple point trajectory is very close to the wedge surface. Note that in Fig. 18 that the Mach stem is curved even though the reflected shock can be observed.

Ohyagi *et al.* [23] conducted a numerical simulation on the Mach reflection of detonations on wedges using a two-step chemical reaction model and the Flux-corrected Transport method. The mixture used in the simulation is $2H_2 + O_2 + 7Ar$. The numerical Schlieren image and soot track for a wedge angle of 20° are shown in Figs. 19 and 20. The trajectory of the triple point can be identified in the numerical smoked foils of Figs. 21 and 22. However, a Mach reflection cannot be clearly identified in the numerical Schlieren images and soot tracks for a 10° wedge. The numerical Schlieren images and soot tracks for a 10° wedge shown in Figs. 20 and 22 show a slightly curved front and the Mach stem and the reflected shock is not clearly defined. The results of their study are found to be in agreement with the study by Guo *et al.* [12]

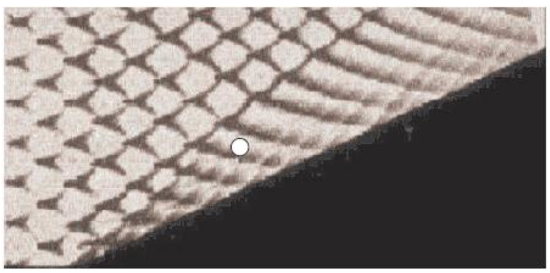

Figure 19: Numerical Schlieren Image for a 20° wedge*[23]*

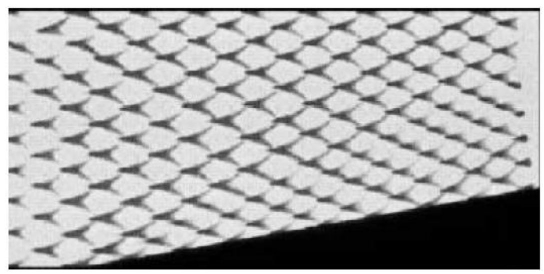

Figure 20: Numerical Schlieren Image for a 10° wedge *[23]*

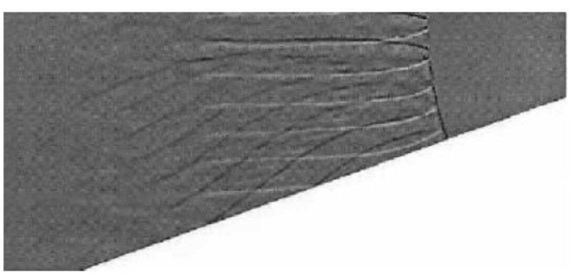

Figure 21: Numerical Soot Track for a 20° wedge*[23]*

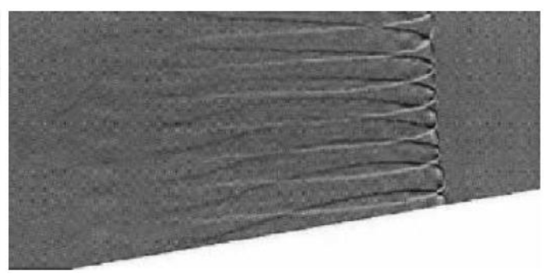

Figure 22: Numerical Soot Track for a 10° wedge *[23]*

Numerical simulations of Mach reflection of cellular detonations using a two-step chain-branching reaction model was also carried out by Li *et al.* [11] They also showed that for small wedge angles, the Mach stem is curved and becomes a continuous front, rather than an abrupt kink of a triple shock configuration. Similar results were also observed in the experimental study by Fortin *et al.*

[10] [24] Acetylene-oxygen mixture with 70% argon-dilution was used and the Schlieren photographs for 10° and 35° are shown in Figs. 23 to 24. For small wedge angles ≲20°, Fortin *et al.* found that the Mach stem becomes curved and merges smoothly with the incident detonation. The triple point becomes dispersed and the reflected wave degenerates into a series of compression waves as the incident detonation intersects continuously with the Mach stem.

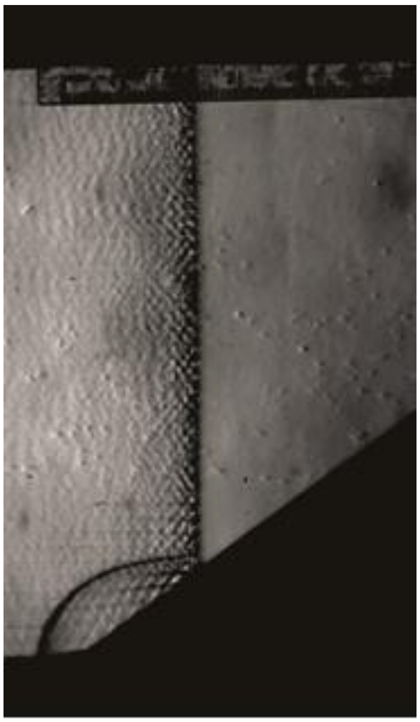

Figure 23: Detonation wave in $C_2H_2 + 2.5O_2$ + 70% Ar over a 35° wedge*[24]*

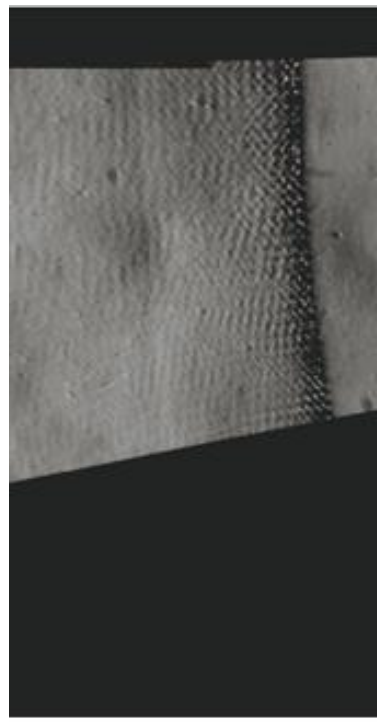

Figure 24: Detonation wave in $C_2H_2 + 2.5O_2$ + 70% over a 10° wedge*[24]*

Almost all the previous studies on Mach reflection of cellular detonations are carried out in a two-dimensional wedge. There appears to be no study on detonations in a three-dimensional conical channel. The present study on the propagation of a detonation in a conical tube is carried out with the objective of investigating a three-dimensional geometry. Conical tubes with a small angle of convergence are used in an attempt to generate a smooth converging front rather than the triple shock configuration. The total cone angles used in the present study are 6° and 10° and experiments were carried out using stoichiometric acetylene-oxygen mixture ($C_2H_2 + 2.5O_2$) and also stoichiometric acetylene-oxygen mixture with 70% argon dilution ($C_2H_2 + 2.5O_2 + 70\%\ Ar$) Experiments are carried out at low initial pressure to permit smoked foils to be used to investigate the cellular structure of the converging detonations.

Chapter 2 : Experimental Details

The experiments are carried out in a steel cylindrical detonation tube which has two sections: a constant area section followed by a conical converging section at the end. A schematic of the experimental setup is shown in Fig. 25.

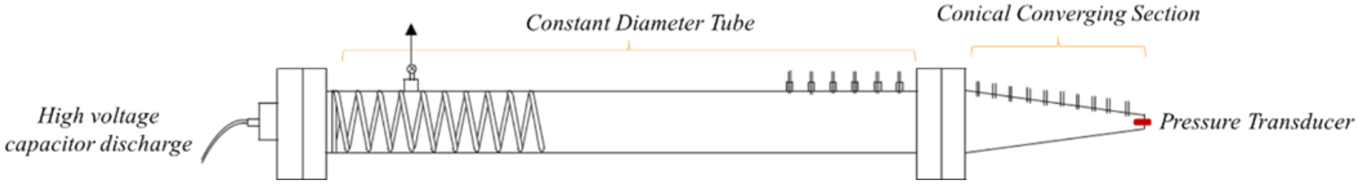

Figure 25: Experimental Setup: Detonation Tube

The constant area section has an inner diameter of 6.35 cm (or 2.5 inches) and a length of 3 meters to ensure a fully developed, steady C-J detonation wave is formed prior to its entry into the converging section. The initiation of a detonation wave is achieved using a high voltage capacitor discharge at the front end of the tube. The ignition circuit diagram is shown in Fig. 26.

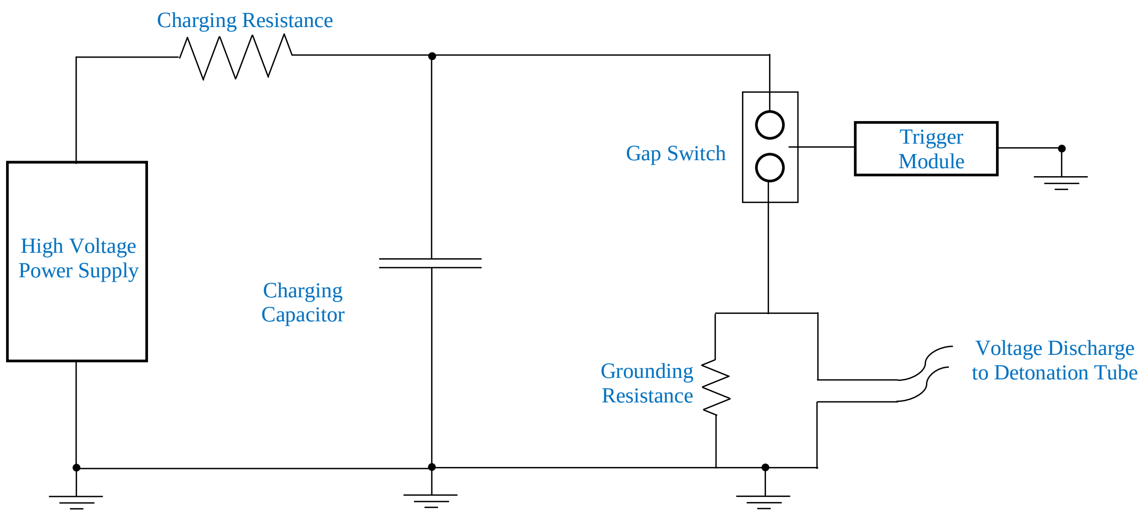

Figure 26: Ignition Circuit Diagram

To facilitate the formation of the detonation wave, a Shchelkin spiral of length of 1.5 m is inserted into the ignition end of the tube. The detonation propagates through the constant area section prior to entering the conical converging section.

Acetylene-oxygen mixture, $C_2H_2 + 2.5O_2$, and stoichiometric acetylene-oxygen mixture with 70% argon-dilution, $C_2H_2 + 2.5O_2 + 70\%$ Ar, are used. The initial pressure ranges of the two mixtures are as follows:

- $C_2H_2 + 2.5O_2$: 0.5 kPa < P_o <10 kPa
- $C_2H_2 + 2.5O_2 + 70\%$ Ar: 4 kPa < P_o <16 kPa

Using small cone angles $\lesssim 20°$, a smooth converging front can be obtained. In the present study, we use small cone angles of 10° and 6°. The conical section converges to a finite radius of 0.635 cm for the 10° cones and 0.254 cm for the 6° cones, respectively. For practical reasons, the conical tubes terminate at some small finite diameter to permit a pressure transducer to be placed to measure the reflected pressure of the converging wave.

Ionization probes are spaced periodically along the constant area section as well as the converging section of the tube. The ionization probes spacing is 15 cm apart in the constant area section and in the conical section, the ionization probes are spaced closer together at 2-3 cm apart. From the time of arrival from the ionization probes, the detonation trajectory and velocity can be obtained.

The reflected detonation pressure at the end of the conical section is measured using a pressure transducer placed at the end of the conical tube. The pressure transducer used is a PCB Piezotronics 113A24 Pressure Sensor. Because the relatively size of the pressure transducer and small diameter of the conical tube, it is not possible to install pressure transducers along the conical tube.

Smoked mylar foils are used, both in the constant area section as well as in the conical section to record the cellular structure of the detonation wave.

Chapter 3 : Results & Discussions

The detonation trajectory can be obtained from the times of arrival of the detonation wave from the ionization probes. A typical detonation trajectory is shown in Fig. 27 that shows the trajectory for the $C_2H_2 + 2.5O_2 + 70\%\ Ar$ at initial pressure of 6 kPa at 6° angle of convergence. The portion to the left of the origin corresponds to the constant area section of the tube prior to the conical section. The extension of the trajectory in the constant area to the conical section is indicated by the dotted line in the *x*-*t* diagrams.

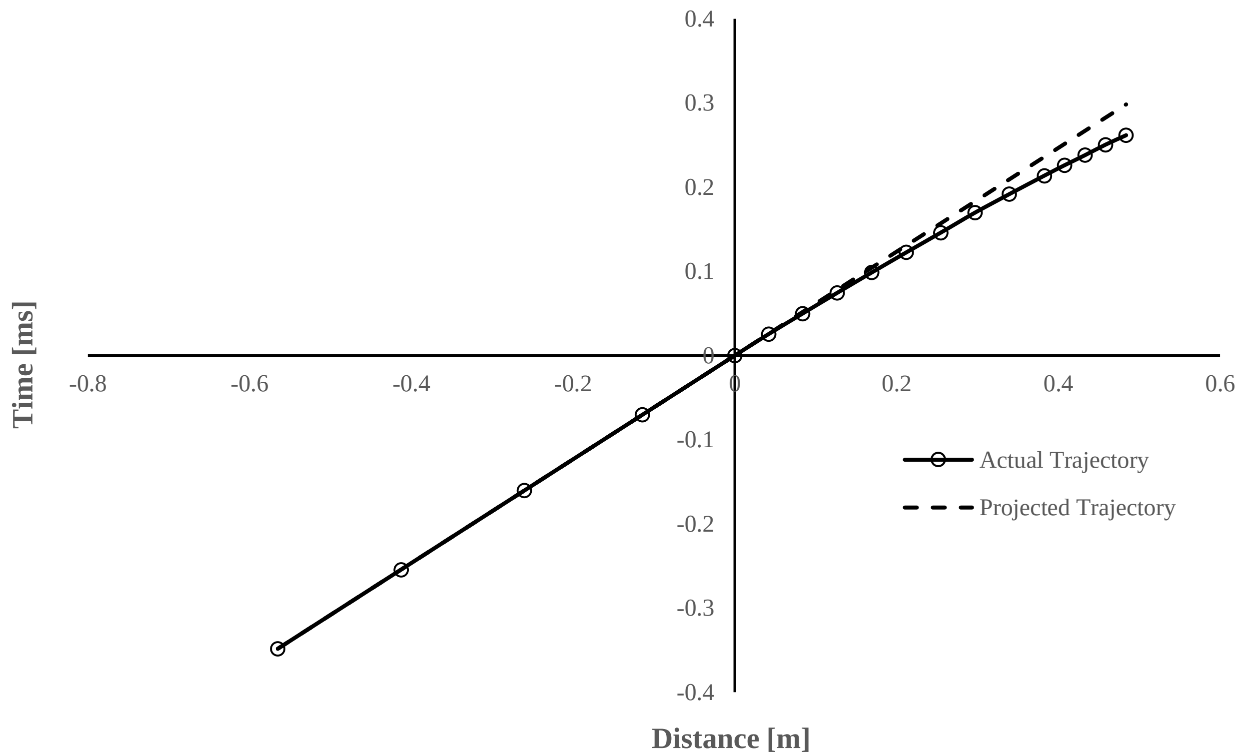

Figure 27: *x*-*t* Diagram for C_2H_2+2.5O_2+70% Argon of 6° Convergence at 6 kPa

Fig. 28 show the trajectories for the same argon-diluted mixture at initial pressure of 6 kPa for the 10° angle of convergence.

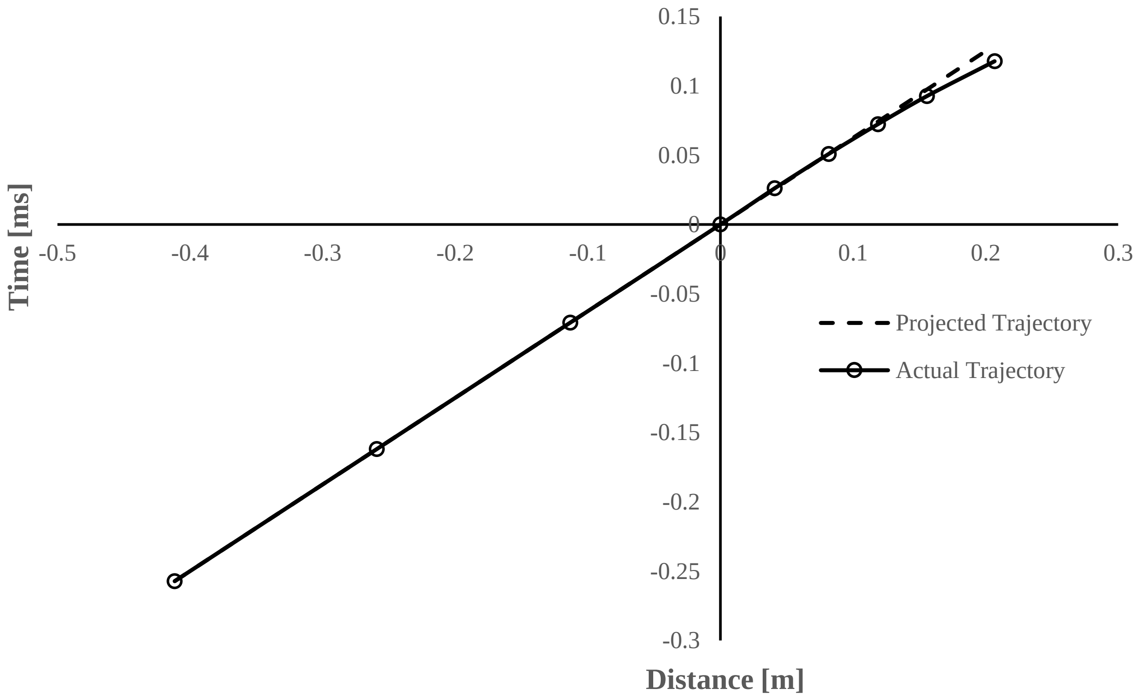

Figure 28: *x-t* Diagram for C_2H_2+2.5O_2+70% Argon of 10° Convergence at 6 kPa

The trajectories indicate an acceleration in the conical section. The degrees of overdrive at the end of the converging section are found to be 1.24 and 1.27 respectively for 10° and 6° conical tube. A greater degree of overdrive is observed for the 6° cone due to a smaller area at the end of the conical section

From the trajectories, the variation of the detonation velocity in the conical section can be obtained. The velocity for the stoichiometric undiluted mixture at 6° angle of convergence is shown in Fig. 29.

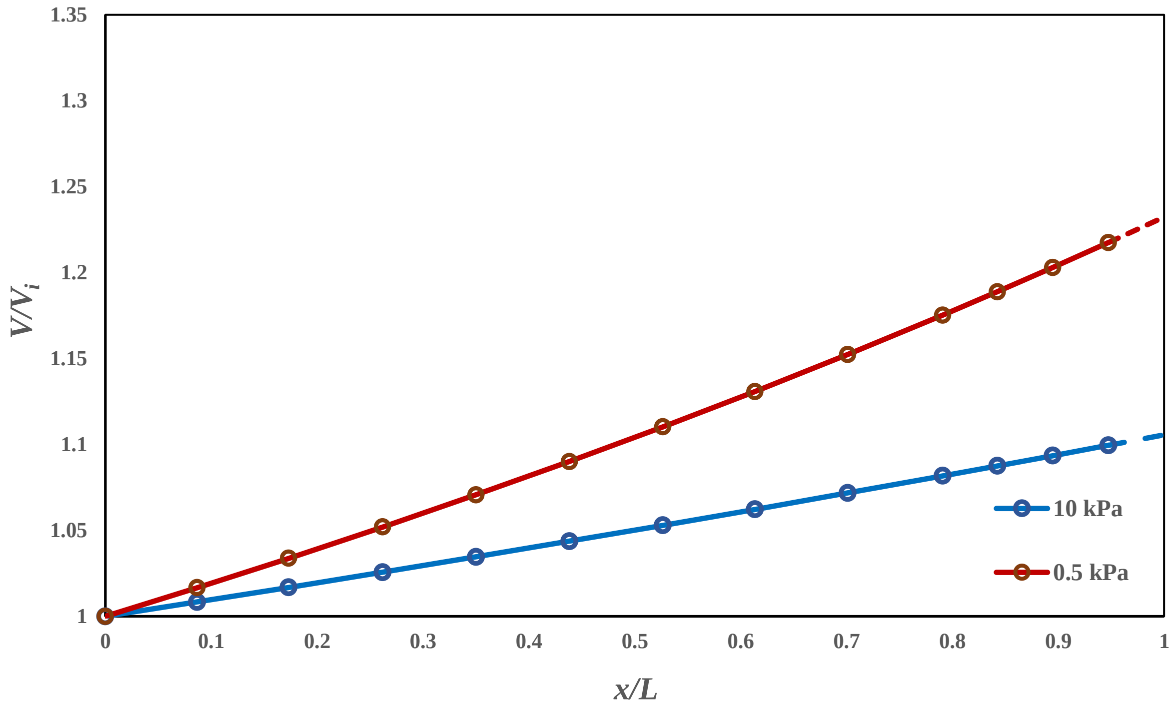

Figure 29: Velocity Profile for C_2H_2+2.5O_2 of 6° Convergence at Different Initial Pressure

The *y*-axis represents the local detonation velocity normalized by the initial velocity at the entrance to the conical section. The *x*-axis represents the distance from the entrance of the conical section normalized by the entire length of the conical section, *L*. The curves indicate the detonation wave accelerates continuously and becomes more and more overdriven as the area converges. A greater increase in velocity is observed at lower initial pressure of 0.5 kPa as compared to the result for higher initial pressure of 10 kPa. The maximum degree of overdrive at the end of the cone at initial pressure of 0.5 kPa is found to be 1.24 while that at higher initial pressure of 10 kPa is found to be 1.10.

A similar result is obtained for the argon-diluted mixture in Fig. 30.

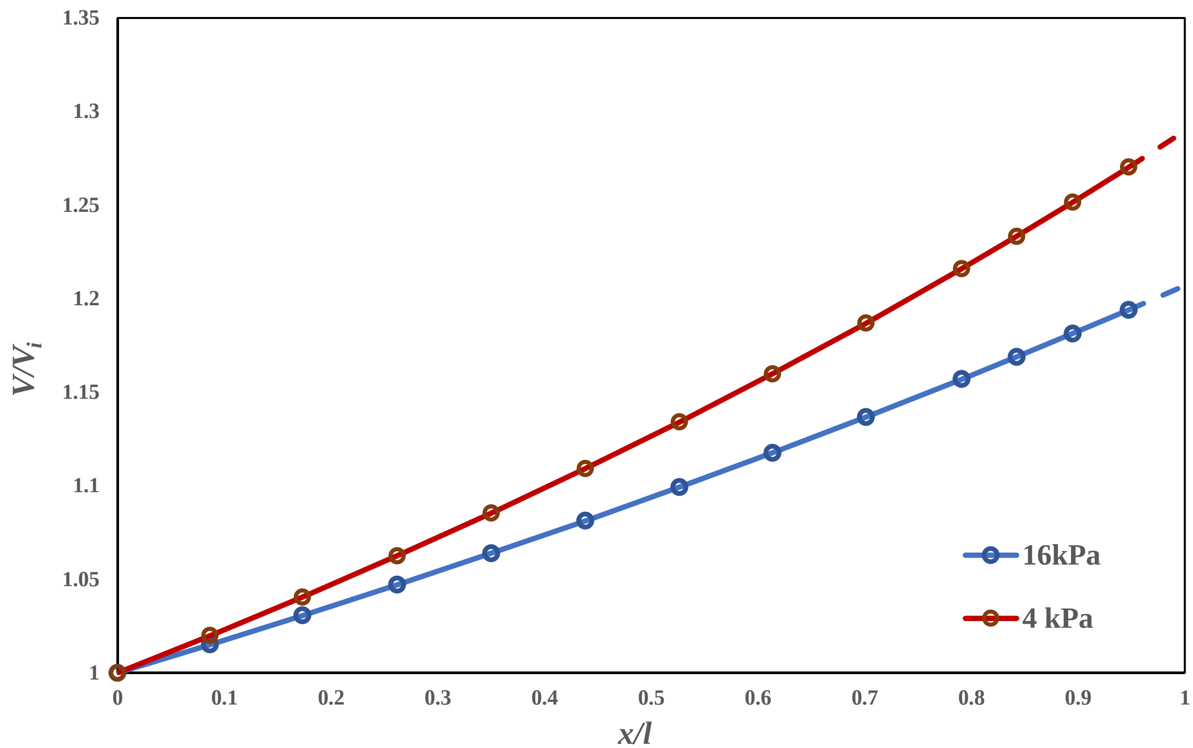

Figure 30: Velocity Profile for C_2H_2+2.5O_2+70% Ar of 6° Convergence at Different Initial Pressures

From Fig. 30 we notice a greater increase in velocity is obtained for the diluted mixtures. Also, a higher degree of acceleration is obtained for lower initial pressure of 4 kPa than for 16 kPa. The maximum degree of overdrive for the argon-diluted mixture at initial pressure of 4 kPa was found to be 1.28 compared to that for the undiluted mixture at initial pressure of 0.5 kPa of 1.23.

It may be concluded from the present results that higher degree of acceleration in the conical tube in obtained from the less sensitive argon-diluted mixture and at lower initial pressures. This may be due to the fact that the more sensitive undiluted, the propagation of the detonation wave is more dominated by the chemical energy release than by the adiabatic compression due to area convergence on the converging channel.

The detonation structure in the constant area section and in the converging section is obtained using smoked mylar foils, as shown in Fig. 31. In each experiment, thin smoked mylar foils are coiled up and inserted into the tube. The first piece on the leftr egisters the cellular structure of the detonation wave in the constant area section, and the second piece registers the cellular structure in the conical section.

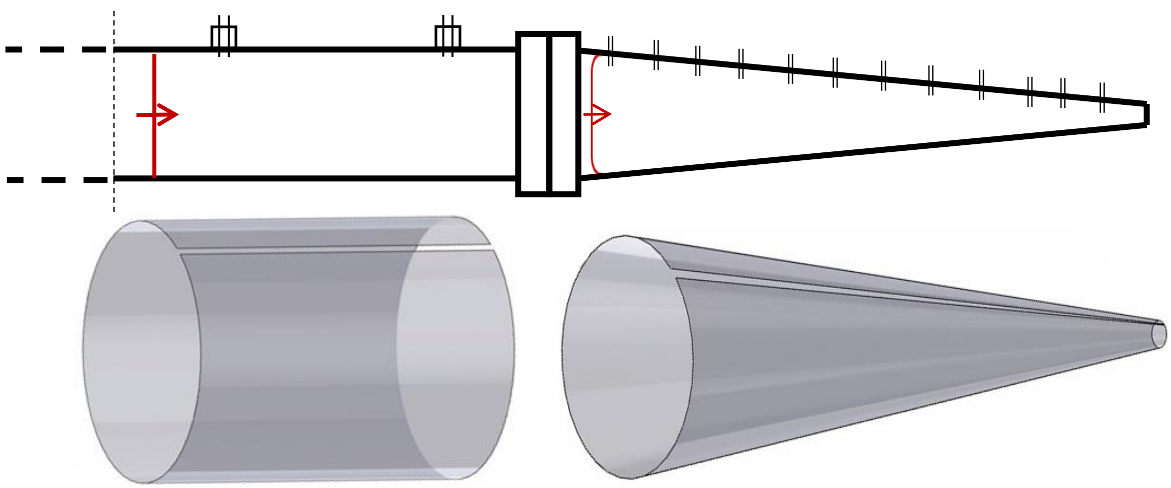

Figure 31: Smoked Foils in the Detonation Tube

Typical smoked foils are shown in Fig. 32 that shows the smoked foils for the $C_2H_2 + 2.5O_2 + 70\% Ar$ at initial pressure of 6 kPa for the 10° conical tube.

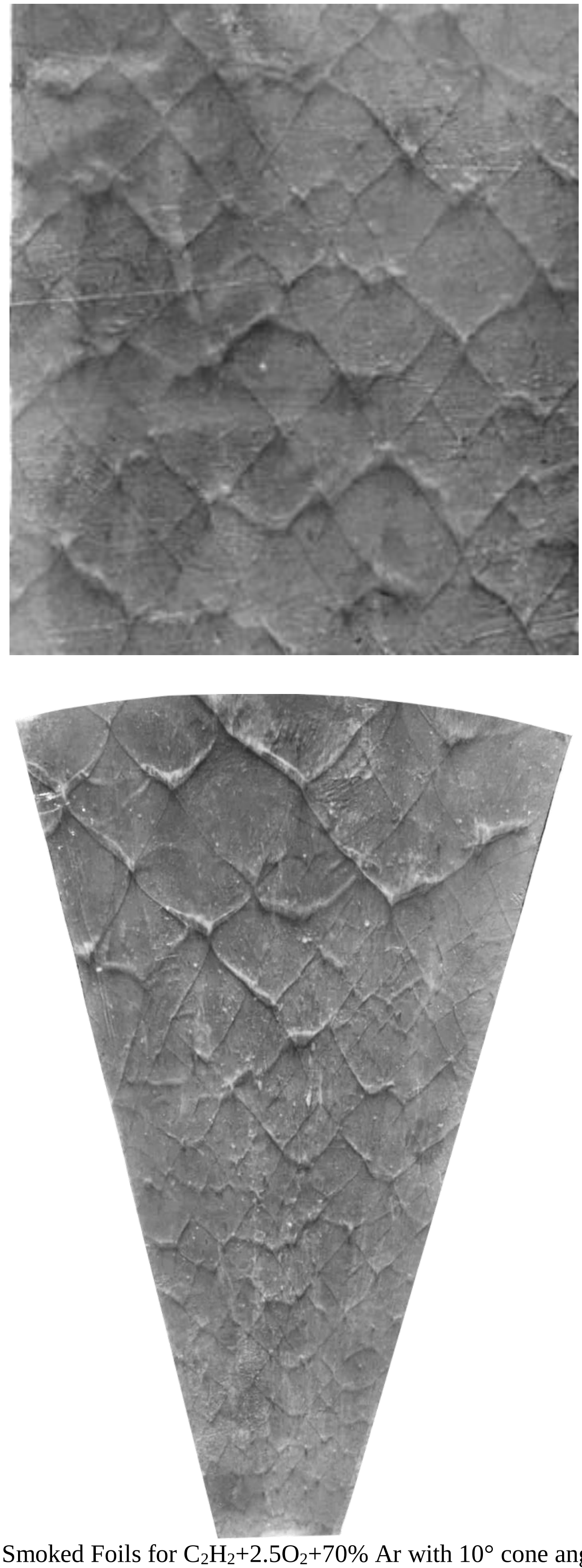

Figure 32: Smoked Foils for C_2H_2+2.5O_2+70% Ar with 10° cone angle at 6 kPa

In the constant area section, the cellular structure is relatively constant with no obvious change in cell size. The average cell size was found to be approximately 21 mm which agrees with the previously published data of 23 mm [25]. This represents the cell structure of a steady, fully-developed detonation before it enters the conical section. In the beginning of the conical section, the cell size is comparable to that in the constant area section, but as the detonation propagates further, there is a continuous decrease in cell size all the way until the end. This indicates that the detonation wave amplifies and becomes increasingly overdriven as the area converges.

The variation in cell size measured from the smoked foils in the conical section are shown in Figs. 33 and 34. The origin corresponds to the entrance of the conical section. The vertical axis represents the ratio of the cell size in the converging section, λ, normalized by the initial cell size, λ_i , in the constant area section. The horizontal axis represents the distance from the entrance of the conical section, x, normalized by the entire of the conical section, L.

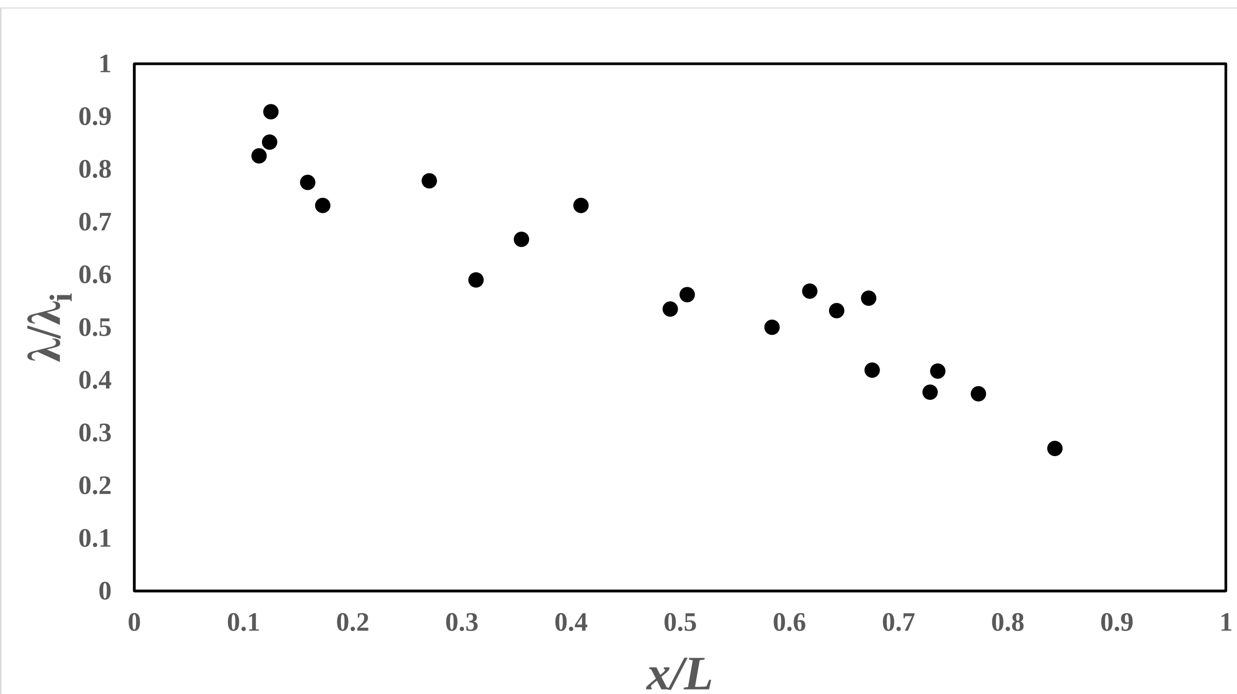

Figure 33: Influence of Area Convergence on Cell Size for C_2H_2+2.5O_2 of 6° Convergence at 0.7 kPa

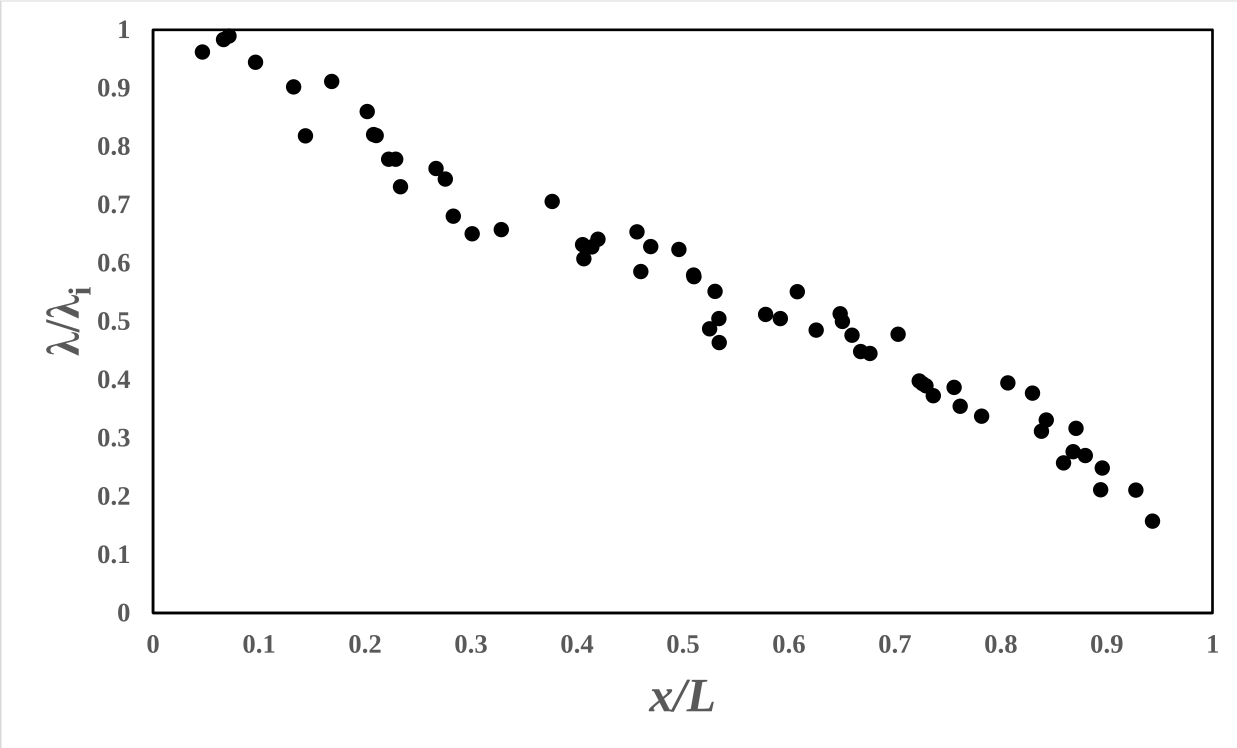

Figure 34: Influence of Area Convergence on Cell Size for C_2H_2+2.5O_2+70% *Ar* of 6° Convergence at 6 kPa

It can be seen that the ratio of the cell size decreases continuously with radius in the converging section shown in both figures. This indicates that the detonation is progressively more overdriven, in contrast to the step increase from multiple Mach reflections where the change of overdrive would be periodic and abrupt.

The pressure at the end of the conical section is measured by a pressure transducer. Figs. 35 and 36 show the reflected pressure ratio at the end of the conical section for the stoichiometric undiluted acetylene-oxygen mixture.

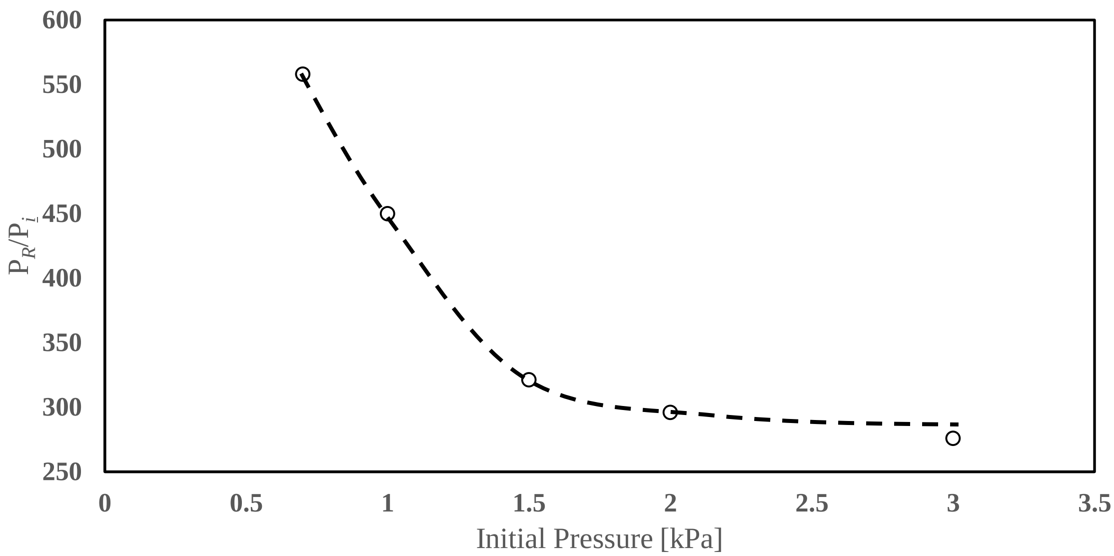

Figure 35: Reflected Pressure Ratio vs. Initial Pressure for $C_2H_2+2.5O_2$ at 10°Convergence

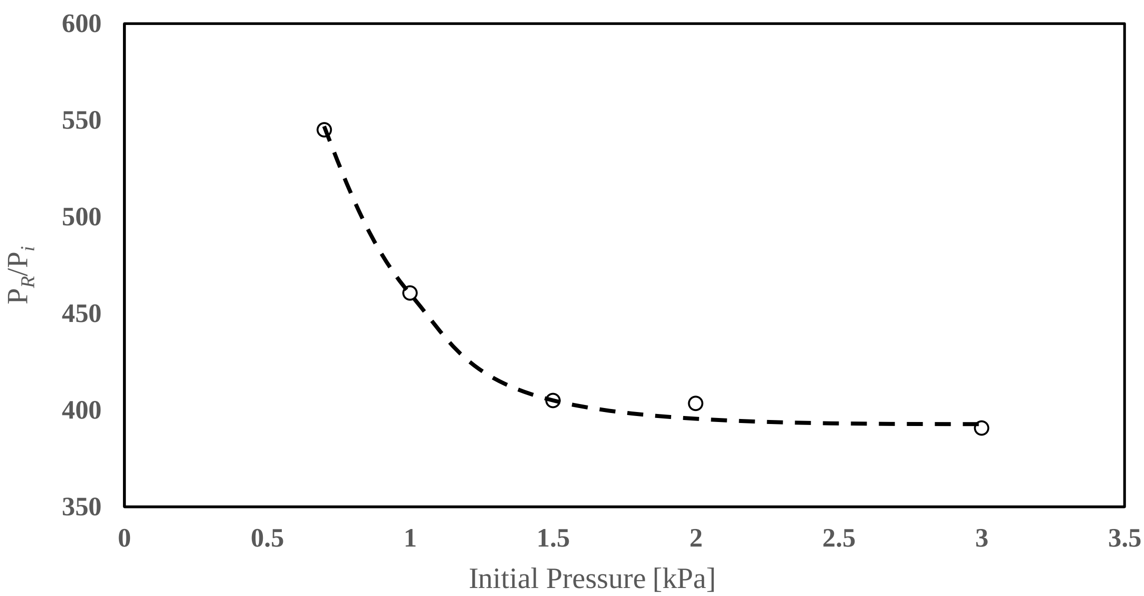

Figure 36: Reflected Pressure Ratio vs. Initial Pressure for $C_2H_2+2.5O_2$ at 6° Convergence

The figures indicate very little change in the reflected pressure ratio at initial pressures above 2 kPa but there is a more pronounced increase at lower initial pressure.

Figs. 37 and 38 show the changes in reflected pressure ratio pressure for both cone angles for the argon-diluted mixture.

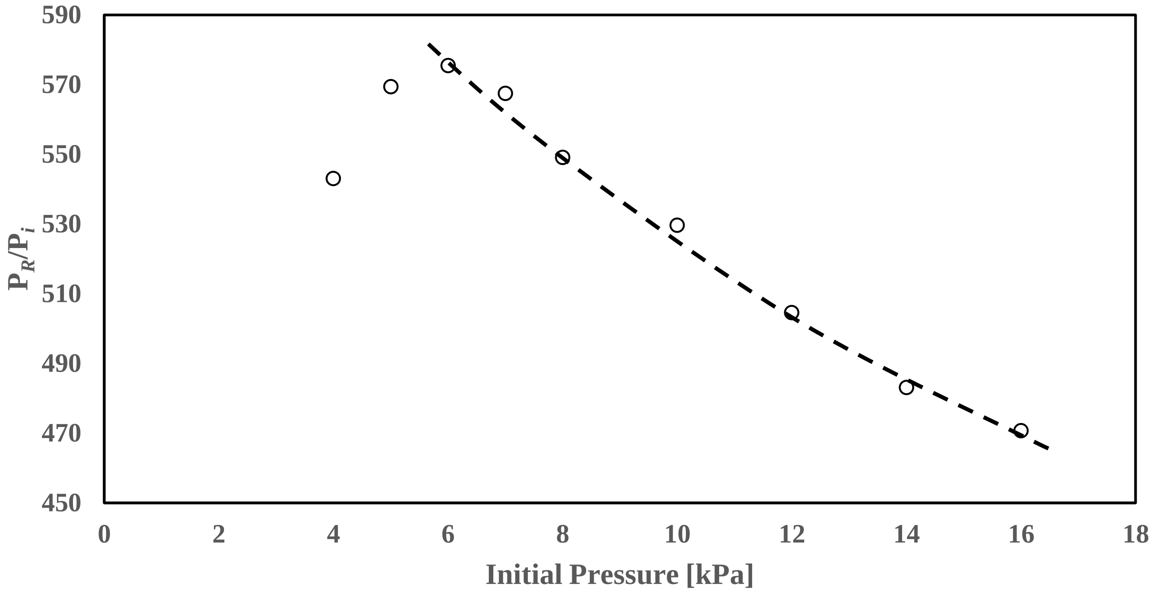

Figure 37: Reflected Pressure Ratio vs. Reciprocal of Initial Cell Size for C_2H_2+2.5O_2+70% Argon at 10° Convergence

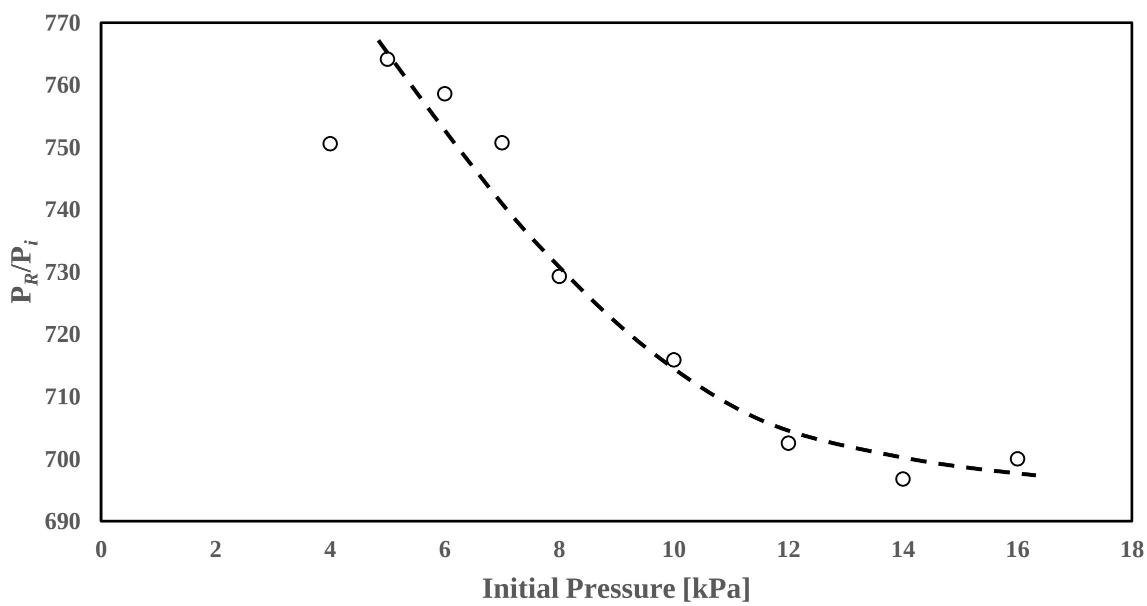

Figure 38: Reflected Pressure Ratio vs. Reciprocal of Initial Cell Size for C_2H_2+2.5O_2+70% Argon at 6° Convergence

Unlike the case for the undiluted mixture, the reflected pressure ratio increases progressively as initial pressure decreases within the entire range. However, at the lower end of the initial pressure range, there is a decrease in the reflected pressure ratios. This could be due to the fact that at very low initial pressure, the cell size gets very large, possibly of the order of the diameter of the PCB pressure transducer itself, thus giving large fluctuations.

Chapter 4 : Conclusion

The effect of area convergence on the propagation of detonation waves in a conical converging channel with small angles of convergence has been investigated in this present research. The cell size, velocity and reflected pressure of the detonation wave were measured as it converges at different initial pressures using stoichiometric acetylene-oxygen mixtures with and without argon-dilution. Two cone angles of 6° and 10° angles are used.

The velocity measurement shows a continuous increase in velocity as the detonation propagates the conical section, indicating it becomes more overdriven and the increase is more pronounced towards the end of rather than the beginning of the conical channel. Maximum degrees of overdrive of 1.27 and 1.30 were obtained for the undiluted and argon-diluted mixture. The amplification is also more pronounced for lower initial pressure and for the argon-diluted mixture, rather than for the undiluted mixture at higher initial pressure. The smoked foils also show a continuous decrease in cell size by the factor 10, with no distinct Mach stem and triple point trajectory observed. This indicates a smooth curved detonation wave front is obtained. The reflected pressure measurement indicates pressure increases at the end of the conical section. Therefore, it can be concluded that a continuously amplification of a detonation wave with a curved wave front can be obtained in a small angle conical tube.

References

[1] J. H. S. Lee and B. H. K. Lee, "Cylindrical Imploding Shock Waves," *Physics of Fluids,* vol. 4, pp. 2148-2152, 1965.

[2] K. Fujiwara, H. Matsuo and T. Hiroe, "New Methods for Generating Cylindrical Imploding Shocks," *Shock Waves,* pp. 81-86, 1995.

[3] K. Terao and H. G. Wagner, "Experimental study on spherically imploding detonation waves," *Shock Waves,* vol. 1, no. 1, pp. 27-34, 1991.

[4] H. Matsuo, "Cylindrical Converging Shock and Detonation Waves," *Physics of Fluids,* vol. 26, no. 7, p. 1755, 1983.

[5] E. S. Oran and C. R. DeVore, "The Stability of Imploding Detonations: Results of Numerical Simulations," *Physics of Fluids,* vol. 6, no. 1, p. 369, 1994.

[6] W. Chester, "The quasi-cylindrical shock tube," *The London, Edinburgh, and Dublin Philosophical Magazine and Journal of Science,* vol. 45, no. 371, pp. 1293-1301, 1954.

[7] R. F. Chisnell, "The motion of a shock wave in a channel, with applications to cylindrical and spherical shock waves," *Journal of Fluid Mechanics,* vol. 2, no. 03, p. 286, 1957.

[8] G. B. Whitham, "On the propagation of shock waves through regions of non-uniform area or flow," *Journal of Fluid Mechanics,* vol. 4, no. 04, p. 337, 1958.

[9] Z. Jiang, C. L. and Z. F., "Dynamics Characteristics of Spherically Converging Detonation Waves," *Shock Waves,* vol. 16, no. 3, p. 257, 2007.

[10] Y. Fortin, J. Liu and J. Lee, "Mach reflection of cellular detonations," *Combustion and Flame,* vol. 162, no. 3, pp. 819-824, 2015.

[11] J. Li and J. H. S. Lee, "Numerical simulation of Mach reflection of Cellular Detonation," 2015.

[12] C. Guo, D. Zhang and W. Xie, "The Mach Reflection of a Detonation Based on Soot Track Measurements," *Combustion and Flame*, vol. 127, no. 3, p. 2051, 2001.

[13] G. Thomas and W. R.L., "Detonation Interaction with Wedges and Bends," *Shock Waves,* vol. 11, no. 6, p. 481, 2002.

[14] V. A. Belokon, A. I. Petrukhin and V. A. Proskuryakov, "Entrance of a strong shock wave into a wedge-like cavity," *Soviet Journal of Experimental and Theoretical Physics,* vol. 21, no. 33, 1965.

[15] D. A. Russell, "Shock-wave strengthening by area convergence," *Journal of Fluid Mechanics,* vol. 27, no. 2, p. 305, 1967.

[16] R. Setchell, E. Storm and B. Sturtevant, "An investigation of shock strengthening in a conical convergent channel," *Journal of Fluid Mechanics,* vol. 56, no. 3, p. 505, 1972.

[17] R. Setchell, "Shock Tube Investigations of Strong Shock Waves in a Convergent Channel," PhD Thesis, Calfornia Institute of Technology, Pasadena, Calfornia, 1972.

[18] D. Q. Duong and B. Milton, "The Mach reflection of shock waves in converging, cylindrical channels," *Experiments in Fluids,* vol. 3, no. 3, pp. 161-168, 1985.

[19] B. Skews and N. Menon, "An experiment on imploding conical shock waves," *Shock Waves,* vol. 11, no. 4, pp. 323-326, 2002.

[20] B. Milton, "Axisymmetric Shock Wave Reflections," *Handbook of Shock Waves,* pp. 265-318, 2001.

[21] Z. Zhai, L. Cangli, F. Qin, J. Yang and X. Luo, "Generation of cylindrical converging shock waves based on shock dynamics theory," *Physics of Fluids*, vol. 22, 2010.

[22] J. Yang, Z. Yujian and Y. Jiming, "Self-ignition induced by cylindrically imploding shock adapting to a convergent channel," *Physics of Fluids*, vol. 29, 2017.

[23] S. Ohyagi, T. Obara, F. Nakata and S. Hoshi, "A Numerical Simulation of Reflection Processes of a Detonation Wave on a Wedge," *Shock Waves*, vol. 10, no. 3, p. 185, 2000.

[24] Y. Fortin, "Mach Reflection of Cellular Detonation," M. Eng Thesis, McGill University, Montreal, 2014.

[25] M. Kaneshige and J. Shepherd, "Detonation Database," P. 140-152. Graduate Aeronautical Laboratories (Fluid Mechanics), GALCIT, California Institute of Technology, Pasadena, California , 1997.

Appendix

Detonation Trajectories:

Fig. 39 shows the detonation trajectory for the case of $C_2H_2 + 2.5O_2$ at initial pressure of 3 kPa at 6° angle of convergence.

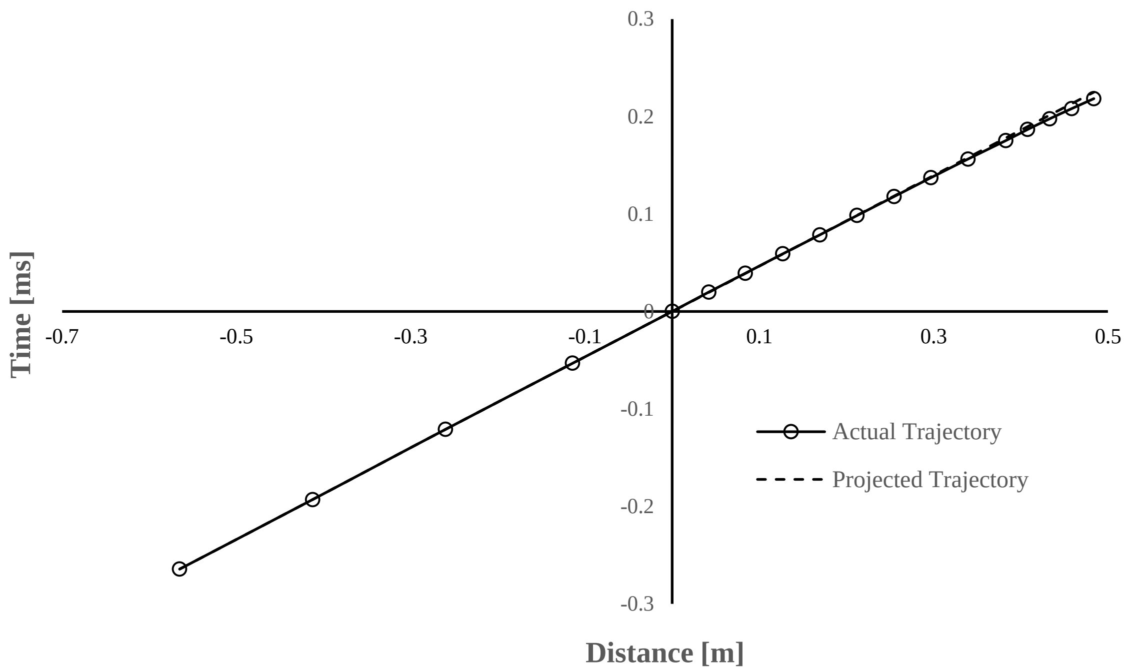

Figure 39: *x-t* Diagram for C_2H_2+2.5O_2 of 6° Convergence at 3 kPa

The trajectory in the constant section is a straight line, indicating a constant detonation velocity. The detonation velocity was found to be 99.1% of the Chapman-Jouguet velocity. The detonation velocity in the conical section is obtained by curve-fitting the trajectory data. The degree of overdrive was found to be 1.10. The trajectories of other experiments with initial pressure above 2.0 kPa is found to be similar to that.

Figs. 40-42 show the detonation trajectory for the case of $C_2H_2 + 2.5O_2$ at initial pressure of 0.5 kPa at 10° and 6° angle of convergence.

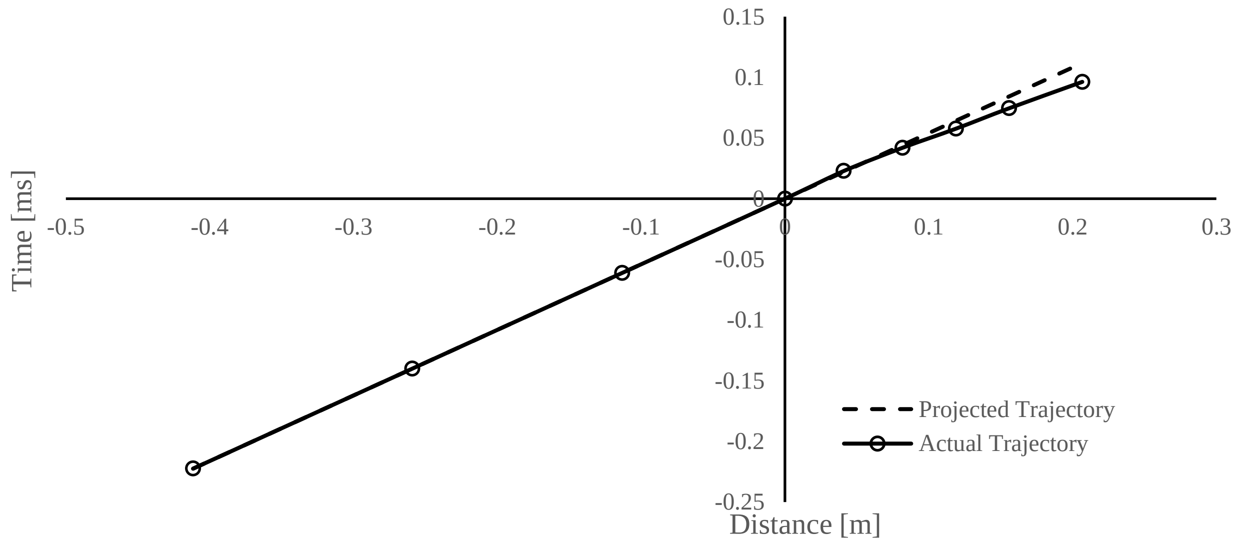

Figure 40: *x-t* Diagram for C_2H_2+2.5O_2 of 10° Convergence at 0.5 kPa

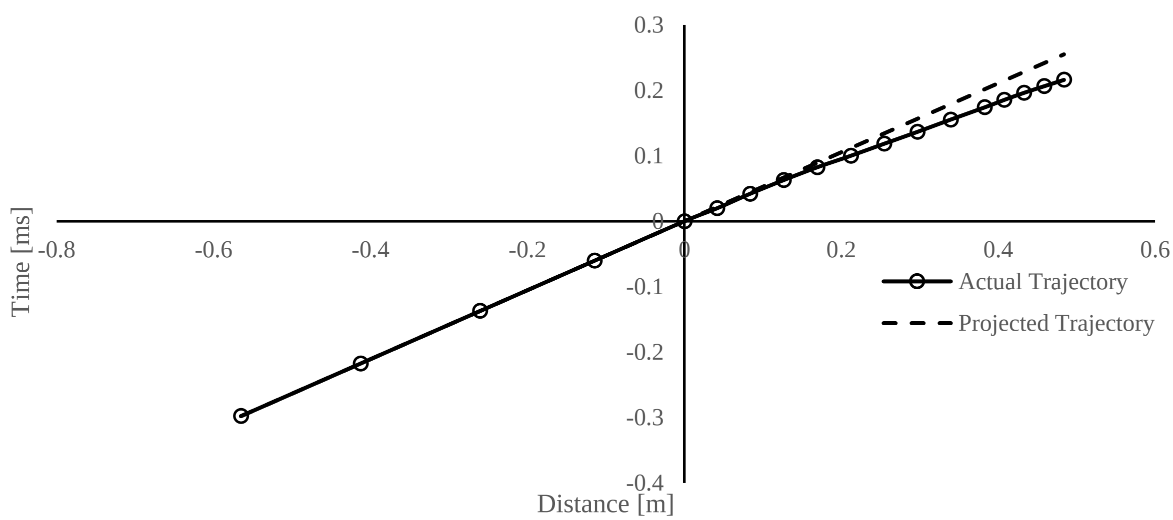

Figure 41: *x-t* Diagram for C_2H_2+2.5O_2 of 6° Convergence at 0.5 kPa

For a lower initial pressure of 0.5 kPa, the maximum velocity obtained at the end of the conical section indicates a more pronounced acceleration as a greater degree of acceleration. From the maximum detonation velocity, the degrees of overdrive were found to be 1.19 and 1.23 for 10° and 6° convergences respectively.

Figs. 42-43 show the detonation trajectory for the case of $C_2H_2 + 2.5O_2 + 70\%\ Ar$ at initial pressure of 16 kPa at 10° and 6° angle of convergence.

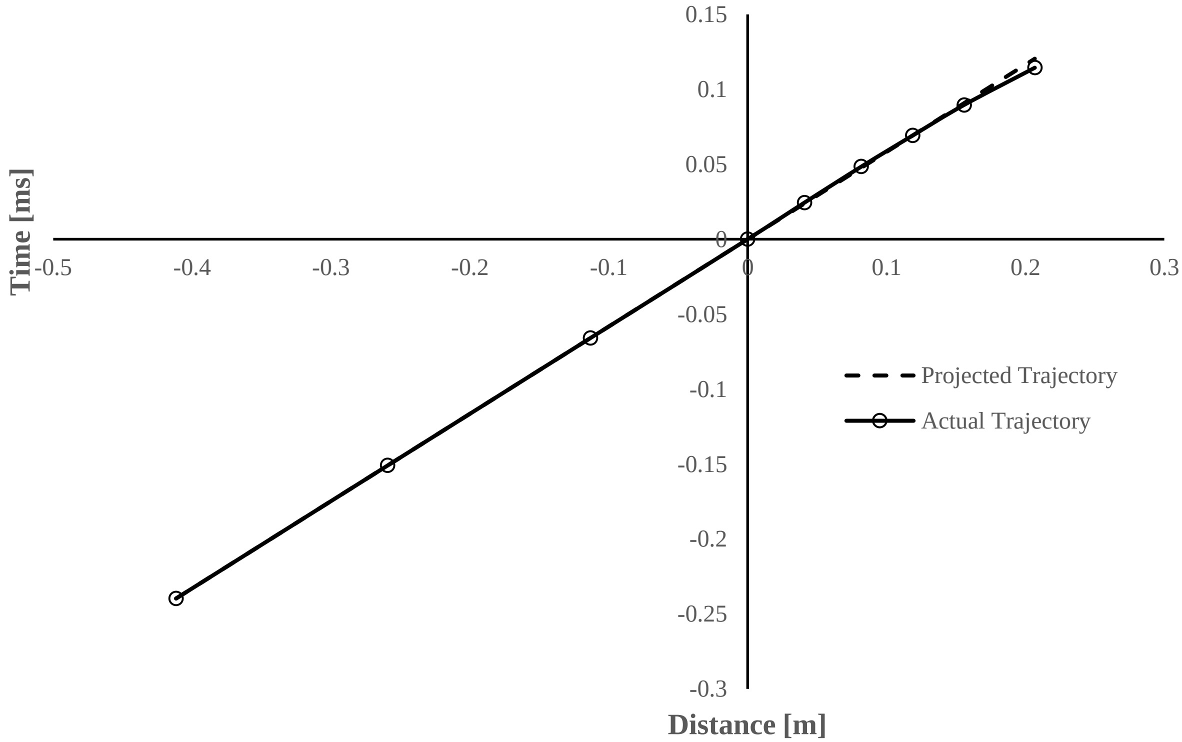

Figure 42: *x-t* Diagram for C_2H_2+2.5O_2+70% Argon of 10° Convergence at 16 kPa

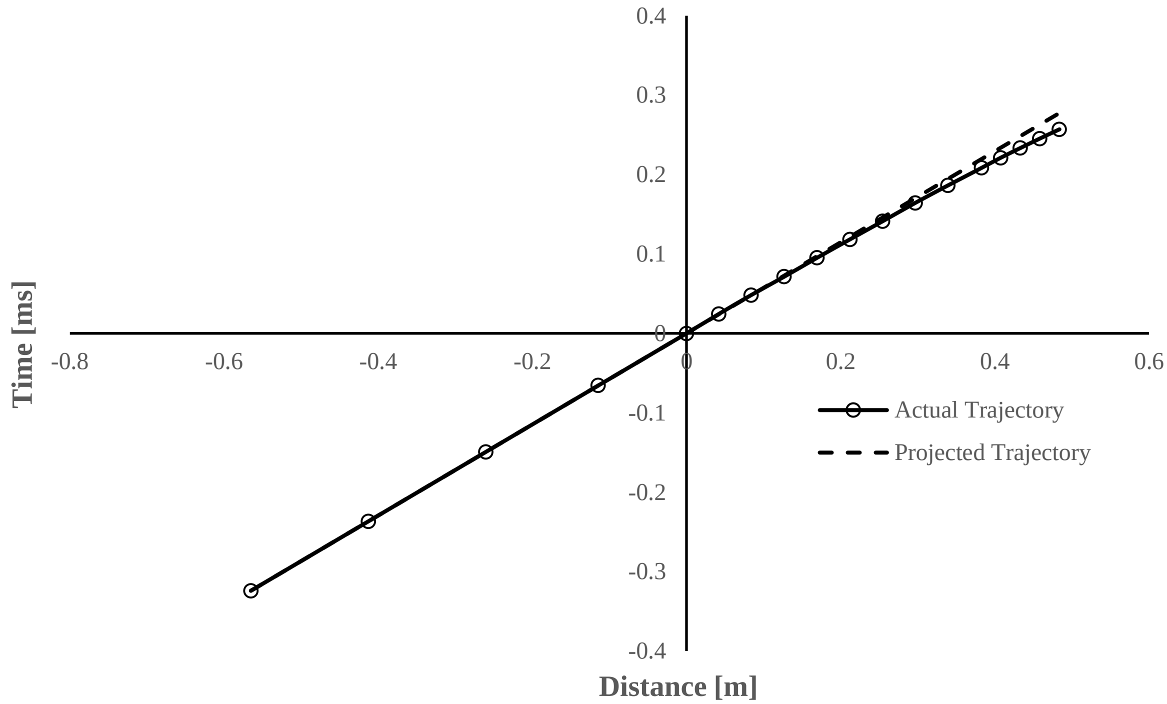

Figure 43: *x-t* Diagram for C_2H_2+2.5O_2+70% Argon of 6° Convergence at 16 kPa

The trajectories indicate an acceleration in the converging section at initial pressure of 16 kPa and the degrees of overdrive at the end of the conical section are found to be 1.15 and 1.20 respectively for 10° and 6° convergences.

Cellular Structure:

Figs. 45-46 show the smoked foils for the case of $C_2H_2 + 2.5O_2$ at initial pressure of 16 kPa at 10° and 6° angle of convergence.

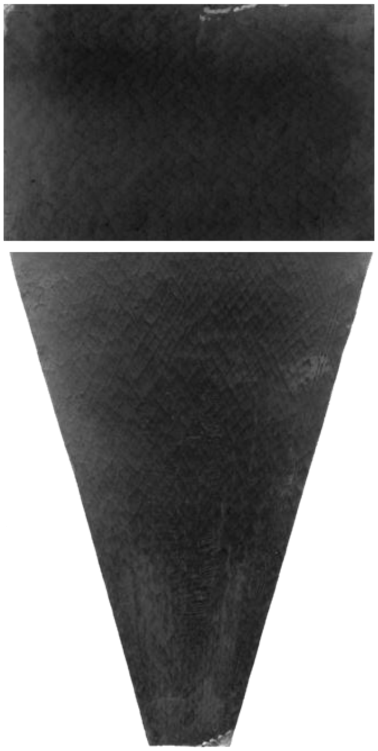

Figure 44: Smoked Foil for C_2H_2+2.5O_2 with 10° cone angle at 3 kPa

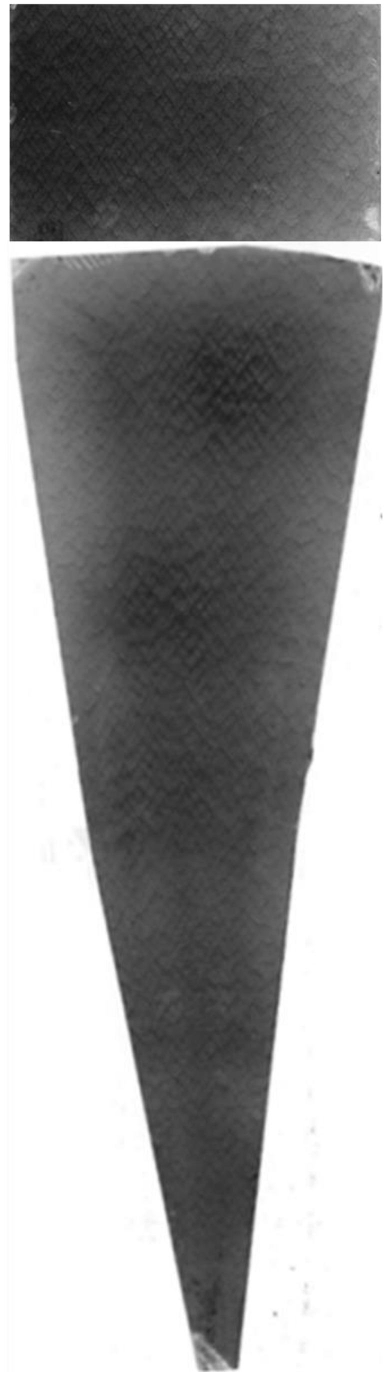

Figure 45: Smoked Foil for C_2H_2+2.5O_2 with 6° cone angle at 3 kPa

It can be seen that the cell sizes in the constant area section at 3 kPa are found to be 6.13 mm and 6.02 mm which agrees with the published data of 5.90 mm at 3.11 kPa [25]. Within the fluctuations in the cell size, a decrease in the cell size due to acceleration in the conical section cannot be clearly observed.

Figs. 46 and 47 show the smoked foils carried out at a lower initial pressure at 1.5 kPa at both cone angles.

Figure 46: Smoked Foil for C_2H_2+2.5O_2 with 10° cone angle at 1.5 kPa

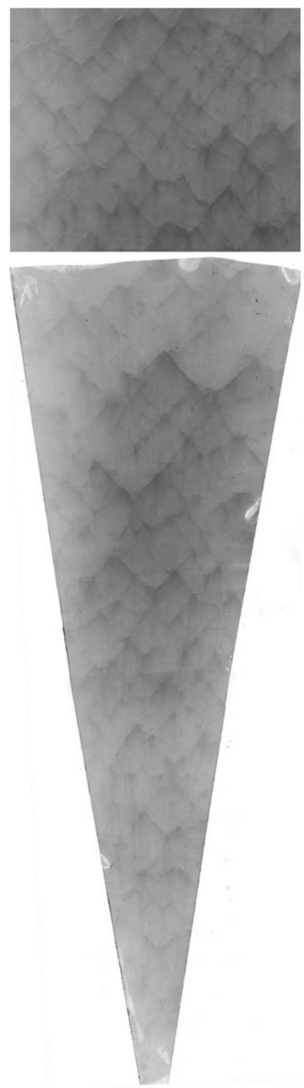

Figure 47: Smoked Foil for C_2H_2+2.5O_2 with 6° cone angle at 1.5 kPa

The initial cell sizes in the constant area section at initial pressure of 1.5 kPa are found to be 22.2 mm and 20.9 mm for 6° and 10° convergences respectively. A lower initial pressure at 1.5 kPa, a decrease in the cell size in the conical section can be observed.

For the argon-diluted mixture, a more regular cellular structure is obtained. The cell sizes in the constant area section for initial pressures of 10 kPa and 6 kPa are found to be 8.2 mm, 18.8 mm which agree with the published data of approximately 9 mm and 20 mm respectively. A pronounced decrease in cell size in the conical converging section at all initial pressures carried out can now be observed for the argon-diluted mixture.

This is demonstrated in Figs. 48 and 49 below at initial pressure of 10 kPa at both cone angles.

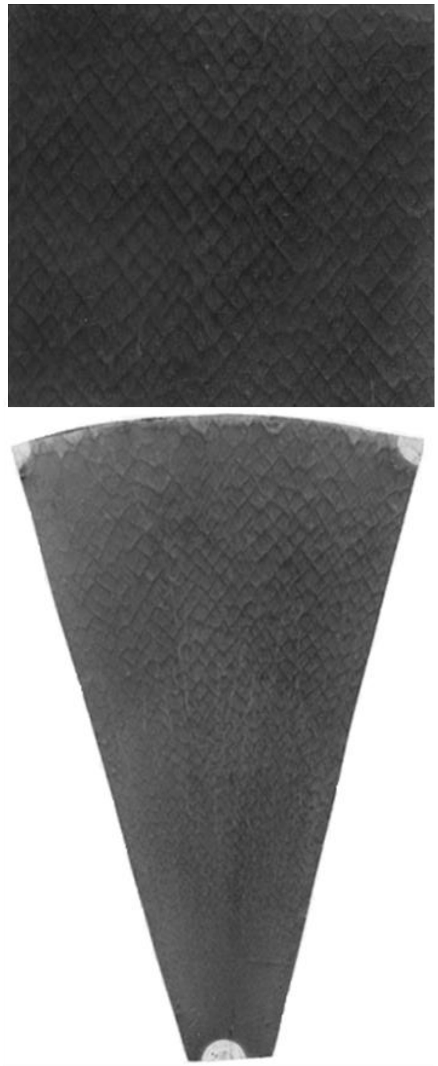

Figure 48: Smoked Foils for C_2H_2+2.5O_2+70% Ar with 10° cone angle at 10 kPa

Figure 49: Smoked Foils for C_2H_2+2.5O_2+70% Ar with 6° cone angle at 10 kPa

Figs. 50 and 51 show the smoked foils conducted for the argon-diluted mixture at initial pressure of 6 kPa at both cone angles.

.

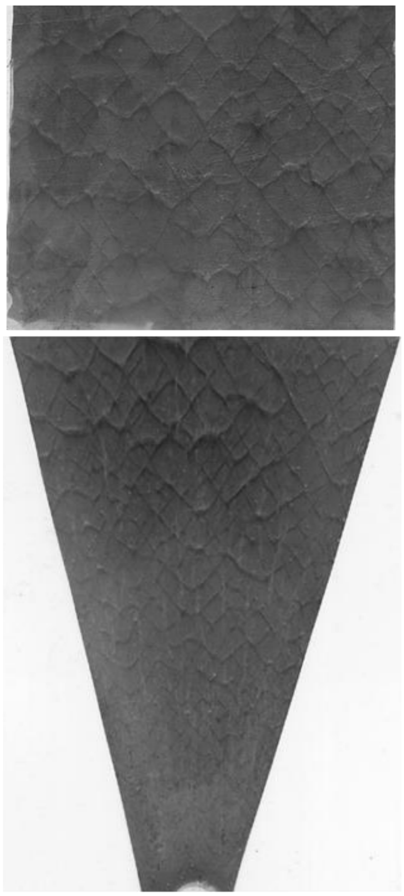

Figure 50: Smoked Foils for C_2H_2+2.5O_2+70% Ar with 10° cone angle at 6 kPa

Figure 51: Smoked Foils for C_2H_2+2.5O_2+70% Ar with 6° cone angle at 6 kPa

It can be seen from Figs. 48 to 51 that as area decreases, the cell size again decreases continuously throughout the converging section.